ATOMISTIC MODELLING TO STUDY PROPERTIES OF GRAPHENE

A DISSERTATION

Submitted in partial fulfillment of the

requirements for the award of the degree

Of

MASTER OF TECHNOLOGY

In

MECHANICAL ENGINEERING

(With specialization in, CAD, CAM& ROBOTICS)

By

MUSE DEGEFE CHEWAKA

DEPARTMENT OF MECHANICAL AND INDUSTRIAL ENGINEERING

INDIAN INSTITUTE OF TECHNOLOGY ROORKEE

ROORKEE-247667, Uttarakhand (INDIA)

MAY, 2016

INDIAN INSTITUTE OF TECHNOLOGY ROORKEE

ROORKEE

CANDIDATE'S DECLARATION

I hereby declare that the work carried out in this dissertation entitled, **"ATOMISTIC MODELLING TO STUDY PROPERTIES OF GRAPHENE"** in partial fulfillment of the requirements for the award of the degree of "Master of Technology" in CAD, CAM & ROBOTICS, submitted to Mechanical and Industrial Engineering, Indian Institute of Technology Roorkee is an authentic record of my own work carried out under the supervision of **Dr. Avinash Parashar** (Assistant professor).

I have not submitted the matter embodied in this Dissertation for the award of any other degree or of diploma to any institute or university.

Date:- ————————

Signature:-————————

Place:-Roorkee

MUSE DEGEFE

Enrolment No. 14538015

CERTIFICATE

This is certified that the above statement made by the candidate is correct to best of my knowledge.

DR. AVINASH PARASHAR

Assistant professor

MIED, IIT Roorkee

Roorkee-*247667*, India

Date: - ———————— *Signature*:- ————————

ACKNOWLEDGEMENT

I would like to express my deep sense of gratitude to my guide **Dr. Avinash Parashar**, Assistant Professor in the department of **MECHANICAL AND INDUSTRIAL ENGINEERING**, **Indian Institute of Technology Roorkee**, for providing me all the necessary guidance and inspirational support throughout this dissertation paper. I feel much honored in presenting this thesis in such an authentic form of complete patience and continual efforts of inspiring excellence from various cooperation and sincere efforts drawn from all sources of knowledge.

I would like to express my profound gratitude to **Dr. Dinesh Kumar**, Professor and Head, of **Mechanical and Industrial Engineering Department**, **Indian Institute of Technology, Roorkee** for providing all the facilities, which would have made it possible for me to complete this dissertation.

I moreover owe a great deal of appreciation to all my faculty members and staff of **Mechanical and Industrial Engineering department, Indian Institute of Technology Roorkee** who have helped me directly or indirectly for the completion of this dissertation.

I would also like to thank, research scholars Rajasekeran and Rajesh Kumar for their help and encouragement at the time of needs and my colleague Anil Gautam who working with me as M-Tech final year.

As a final personal note, I am most grateful to Almighty God for showering blessings on me and my family members who are inspirational to me in their understanding, patience and constant encouragement at a distance.

Financial support from Ethiopian Embassy, Educational Research Council is thankfully acknowledged.

MUSE DEGEFE

ABSTARCT

This thesis addressed that graphene is a regular monolayer of carbon atoms settled in a 2D-hexagonal lattice; that is listed among the strongest material ever measured with strength exceeding more than hundred times of steel. However the strength of graphene is critically influenced by temperature, vacancy defects (VD). Defects are at all believed to worsen the mechanical toughness and reduce the strength of graphene sheet. Revealed boldly that stiffness and strength are the key factors in determining solidity and life span of any technological devices; besides at the time of production defects can change the structural properties of any engineering material. A systematic MD simulation (MDs) study is performed in this thesis toward understanding the defects on the mechanical properties of graphene, that the MD simulations provide important comprehensions. Simulation of sheets with vacancy defects indicates that a single missing atom could diminish the strength by nearly 25%. Also MD based atomistic modeling was performed to predict and quantify the effect of non-bonded interactions on the failure morphology of vacancy affected sheets of graphene. Defective sheet of graphene containing VD was simulated in conjunction with the non-bonded interactions experienced due to the presence of pristine sheet of graphene. In this study, the author, revealed mechanical properties and failure morphology of bi-layer graphene sheets under the influence of single, double and multi-vacancy defects. It was concluded on the basis of atomistic simulations that non-bonded interactions as well as stiffness of pristine graphene sheet has significant impact on the failure morphology of the defective sheet of graphene. Non-bonded interactions in conjunction with defects can be further used for modifying the brittle nature of graphene to ductile.

TABLE OF CONTENTS

LIST OF SYMBOLS

E	Young’s modulus
D	Third order elastic modulus
σ	Stress
ε	Strain
C	Carbon
N	Number of atoms
V	Volume
T	Temperature in Kelvin's
P	Pressure in Pascal
U	Strain energy
Γs	Surface energy density
2a	Crack length
ρ	Crack tip radius
˚A	Angstrom
r	Position vector
Δt	Time step
t	Time
v	Velocity
kB	Boltzmann's constant
m	Mass
f	Force
A	Area

LIST OF ABBREVIATIONS

MD	Molecular dynamics
0d	Zero dimensional
1d	One-dimensional
2d	Two-dimensional
3d	Three-dimensional
QSMD	Quasi-static molecular dynamics
MM	Molecular mechanics
QM	Quantum mechanics
VMD	Visual molecular dynamics
PBC	Periodic boundary conditions
CTE	Coefficient of thermal expansion
CNT	Carbon nanotube
GNR	Graphene nanoribbons
GNS	Graphene nano sheet
GO	Graphene oxide
GRMs	Graphene and related materials
AFM	Atomic force microscope
AFEM	Atomic-scale Finite Element Method
SEM	Scanning electron microscope
SiC	Silicon carbide
TEM	Trans- mission electron microscope
NEMS	Nano-electromechanical system
REBO	Reactive empirical bond order
AIREBO	Adaptive intermolecular reactive empirical bond order
NVE	Constant number of atoms (N), volume (V),and energy (E) ensemble
NVT	Constant number of atoms (N), volume (V), and temperature (T) ensemble
NPT	Constant number of atoms (N), pressure (P), and temperature (T) ensemble

LIST OF TABLES

LIST OF FIGURES

LIST OF PUBLICATIONS

The part of this thesis, contains the paper which was published previously entitled with "Effect of non-bonded interactions on failure morphology of a defective graphene sheet" in the Journal review of IOP publishing Institute of physics.

1. Muse Degefe and Avinash parashar, Effect of non-bonded interactions on failure morphology of a defective graphene sheet: Mater. Res. Express 3 (2016) 045009 (IOP Publishing), status *published.*
2. Muse Degefe and Avinash parashar, "Atomistic modelling to study properties of Graphene". *ASME Conference 2016, for technical presentation IMECE2016-65819, status Abstarct submitted 05 Mar 2016 accepted 12 Mar 2016.*

CHAPTER 1

INTRODUCTION

Graphene is a mixture of closely packed carbon atoms arranged in a two-dimensional (2-D) hexagonal lattice which is bounded together in repeated pattern. It is also an outstanding material lonely with an enormous number of amazing properties which repeatedly gross it into the title of "wonder material" which is a road map on the way to guide the community toward the development of products [1].The remarkable mechanical behavior and properties of graphene-based non material's has concerned with important study concern in recent years, in line for to their encouraging forecasts, now adaptable divisions for example micromechanics [2], microelectronics [3], and thermal [4] application with desired mechanical properties, and electrical conductivities [2-4]. The trial and hypothetical revision of graphene, two-dimensional (2D), is a tremendously growing field of today's condensed matter research. The causes for this is massive methodical attention were diverse, on the other hand one might highlight some key inspirations. Keeping in view of the science based interest generated via graphene and its promising upcoming contribution toward electronic engineering and sensing applications, so group of research effort are steadfast hooked on considering the configuration and properties of graphene in this thesis. Owed toward its excellent mechanical behaviour, thermal and electrical conductivities of graphene could also use for more conventional purposes as compared with carbon nanotubes, which was quiet restricted to aerospace industries. Graphene is known to have very-high stiffness in addition strength until now an extensive scatter have been witnessed in the mechanical properties [1-4].A single sheet of pure graphene sheet was reported to have high young's modulus of about 1.0TPa[1],fracture strength of 130 GPa [1],ultimate tensile strength (σ_{st}) 100GPa [2],thermal conductivity of 5000 W/mK [3-4],shear modulus of 280GPa [5-6],longitudinal sound velocity of 20km/s [5,7-9],melting temperature of 4900K [5,10] and also it has electron mobility of 250,000cm2/Vs at room temperature[1]. Graphene makes experiments possible that give new turns to the wonders in quantum physics application in electrical, mechanical are the most important in microelectronics engineering as a component material ;as a super conducting material; like micro-

chips clear conducting electrode and solar cells[10-14].Because of its special properties, it is increasing the research endeavor to evolve recent engineering applications for instance nano-actuators [15-16],nano-sensors [15, 20], gigahertz oscillators [15, 18], drug deliver[15, 19]. Accounting these nanotechnologies, graphene is also recorded amongst topmost possible nanofillers aimed at emerging as nano composite material thru enhanced properties, thermal and electrical conductivities which put into effect us to look toward it [15, 19, and 20].

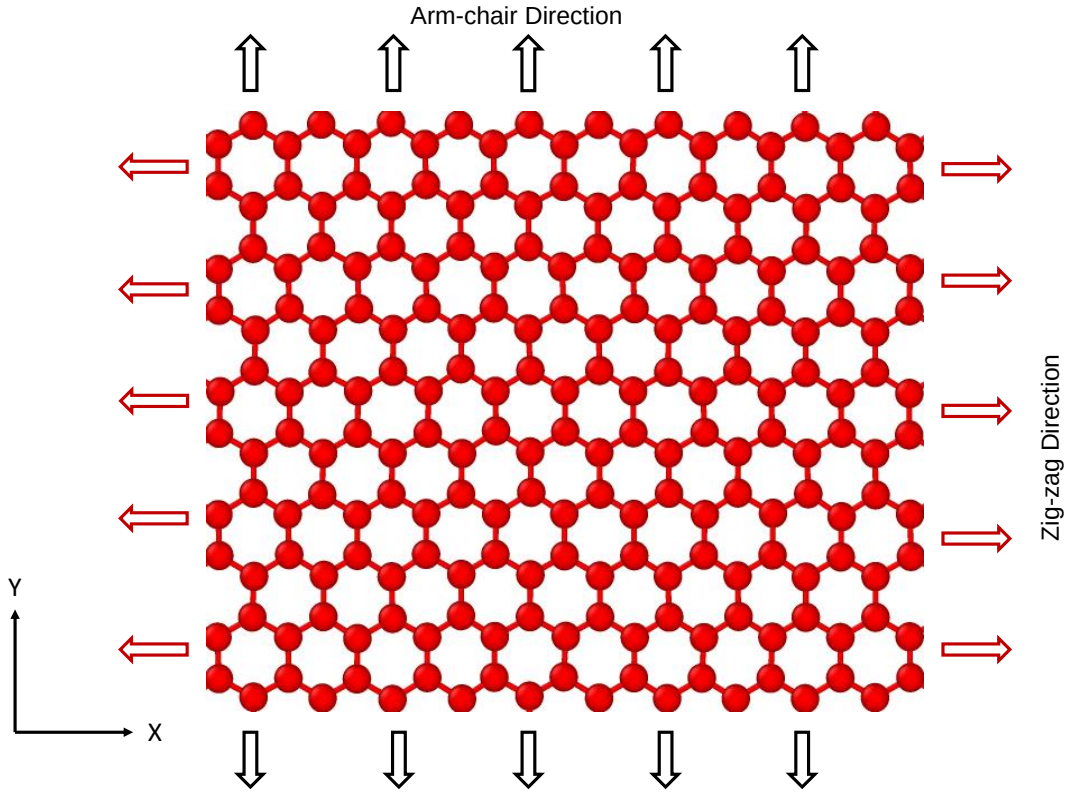

Figure 2. Atomistic modelled of graphene configuration.

Whereas currently reports on graphene are a material that can be utilized in numerous disciplines including, but not limited towards, bio-engineering, amalgamated materials, energy technology and nanotechnology according to previously had done paper by some authors. Still material manufacturing developments and chemical action may familiarize structural defects in graphene; for instance single, di- and multi-vacancies are recently studied by Gorjizadeh et al. [16] validated the conductance drops in defective graphene sheet. Pei et al. [17, 18] premeditated the effect of functionalized clusters proceeding to study properties of graphene. Banhart et al. [19] revised,

conceivable structural defects in graphene and their special effects for its potential applications. Regrettably, there are very few studies of defects on the effects of mechanical properties of graphene and consequently more work is abundantly required. This work presents molecular dynamics simulation exploration taking place for the origination of crack length.

Table 1.List of Properties for a Single Sheet of Graphene

Property	**Value**
Young's modulus [1]	1.0TPa
Rupture strength [1]	130GPa
Tensile strength [2]	100GPa
Thermal conductivity [3-4]	5000w/mK
Shear modulus [5-6]	280GPa
Longitudinal sound velocity [5,7-9]	20km/s
Melting temperature [5,10]	4900K
Specific surface area [11]	2630m^2/g
Optical transmittance [12]	97.70%
High electron mobility [13]	250,000cm^2/Vs

1.1 Production techniques

The industrial intake of graphene materials (GMs) will need enormous measure and less price fabrication techniques, though provided that a stability among comfort of manufacture and last material value, definite as on-request made-to-order properties according to the final use. One advantage of graphene is that, unlike other nano materials, it can be completed on huge and economical scale by means of bottom up (atom by atom growth) or top-down (exfoliation from bulk) techniques. So far, the production methods can be classified into two categories:

- Bottom up methods
- Top down methods

Bottom-up processes inculcates, when graphene is manufactured by a variety of methods, such as:

1. Epitaxial growth on metal Carbides [20]

2. Chemical vapor deposition (CVD) [21]

3. Arc discharge [22]

4. Freeing carbon nanotube's [23] (CNT's)

CVD and epitaxial growth on silicon carbide (SiC) are the most joint and widely used; but they every so often make insignificant extents of huge-size, from defect-free graphene sheet. They may be more applicable than the mechanical cleavage method [24]. The techniques of top-down approach, we start with a bulk material and then break it into smaller parts by means of mechanical, chemical or other forms of energy. A schematic representation of the building of nanostructures with down up and above down lines (besides differences between them) is given at Fig.2.

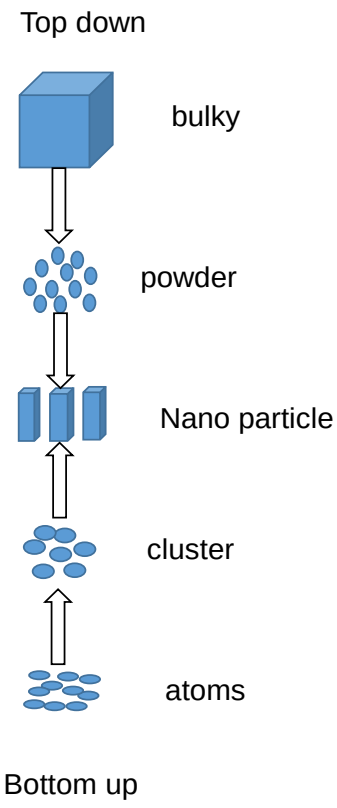

Figure 3.Schematic representation of the building up of nanostructures.

Top-down processes reveal that, graphene sheet can be synthesized/manufactured by several ways; such as,

1. Micromechanical exfoliation of graphite [24]

2. Direct sonication of graphite [25]

3. Chemical reduction of organically treated Graphite Oxide (GO) [26]

4. Thermal exfoliation/reduction of GO [27]

As mentioned above, the micromechanical exfoliation of graphite as a method to produce single graphene sheet is the one that caused the outburst/arisen in this research field in 2004 [24] in upper-down procedures, graphene or sheets are produced by separation/exfoliation of graphite or graphite spin-offs, such as graphite oxide (GO).

Graphene is typically formed from graphite by a top down approach, either by chemical or physical exfoliation [24].In general ,graphene sheets are produced through chemical vapor deposition (CVD) [23] ,mechanical exfoliation [21],chemical exfoliation [21],condensed graphene oxide [21].

1.1.1 Mechanical Exfoliation

Mechanical exfoliation was the unique technique towards preparing graphene. With both sides of highly oriented pyrolytic (thermo chemical decomposition with absence of oxygen or any halogen) graphite adhered by adhesive tape, graphene is obtained through repeated tear, due to the weak van der Waals force in graphite layers. Graphene was first prepared by Novoselov and Geim and their colleagues with this method [28].

1.1.2 Epitaxial Growth Method

SiC is used as input material in this technique. Single or multi-layer graphene is arranged by removal of silicon atoms in the process of sublimation at high temperature. The width is decided by heating temperature, this technique to prepare graphene was first adopted by Berger et al. [29].

1.1.3 Chemical Vapor Deposition

This technique is extra approach that is widely studied and used except redox method. Gaseous carbon source is bubbled into reaction chamber directly, and graphene is obtained due to the precipitation of supersaturated carbon or the surface catalytic cracking of carbon source on metal substrates.

1.2 Applications of graphene as a nano material/nanofiller.

Possible applications of graphene consists of electronics, light processing, energy storage, generators, sensors, plasmonics, meta-materials, along with numerous medical and other industrial processes improved by the use of novel graphene materials. An indication of graphene applications was presented in applied applications; the problem of hydrogen storage and transportation, mostly for usage in mobile applications, must be skilled before hydrogen can become a widespread power source.

1.2.1 Electronic devices

Graphene have already proven for its high potential toward impacting most ICT (information communication technology). The boundless potential of graphene is bear witness by increasing number of chip-producers currently energetic in [30].

1.2.2 Energy Storage and conversion

Storing and converting are essential for energy production and saving. Graphene today also used as energy storage and converter replacing aluminum solar panel in different application.

1.2.3 Sensors

Quickly growing usage of sensors through society and the request for less cost. Improved devices with less power feeding, depend critically on the occurrence of new sensor materials and concepts.

1.2.4 Composites

These applications need little cost, high-progression ability in solvents and polymers and tunable chemical properties. A benefit of graphene over other nano-materials is that it can be formed either by lower-up assembly of smaller atoms and molecules or higher-down exfoliation of graphite masses.

1.2.5 Biomedical Applications

Using nano-technology expected at usage of, diagnosis, intensive care and regulating of biological schemes is called “nanomedicine” [31]. The exceptional properties of graphene deliver principally infinite options for several applications; the biomedical applications of graphene-centered polymer nano-composites. The first report on biomedical application of graphene emerged in 2008 [32, 33], subsequently graphene and graphene-based nano-materials have been utilized in a myriad of bio-applications (e.g., drug and gene delivery, nano-medicine, bio-imaging and potential cancer therapies). Adding to the above; Robust and light weight mixtures would also certify us to build new cars, airplanes, and other structures using less material and energy, and contribute directly to a more sustainable world, see Fig. 3.

Figure 4.Summary uses of graphene in dissimilar subdivisions fluctuating from conductive ink, chemical sensors, light emitting devices, composites, energy, to touch panels and high frequency electronics. (Source: From the Royal Society of Chemistry), volume 7 page 4608.

1.3 Definition of problem

1.3.1 Why atomistic modelling

Failure elements of any material eventually tips to its total configuration and intended function. Computational modeling, in particular atomistic and molecular simulation, is becoming increasingly important in the development new technologies. At nanoscale, the effects of single atoms, individual molecule, or nano structural features may dominate the material behavior. Thus novel modeling and simulation approaches are a vital component in enabling the engineering design process. Atomistic models, by providing a material description that starts at a fundamental scale, are thus expected to be important not only for scientists but also for engineers. In addition that atomistic modeling provides an essential narrative of the materials behavior and materials deformation phenomena. The atomistic modelling includes the physical basic numerical implementation and examples of atomistic models for specific materials, as well as a brief introduction into multi-scale simulation methods. We also review analysis methods, in particular picturing schemes that can be used to cite useful information from large atomistic systems. The significance of the atomistic viewpoint for failure processes and the enormous computational burden associated with such problems makes modeling and simulation of failure a promising and exciting area of research on material.

1.3.2 Why vacancy defect

Graphene is the toughest material; however its performance is pointedly weakened by vacancy defects. So far the researchers used molecular dynamics simulations to investigate mechanical properties like tensile behavior of a graphene which contains a single vacancy (SV), double vacancy (DV) and multiple defect (MV) where the stress concentration around the vacancy defect leads to material distortion/alteration in shape. On the other hand, both material production methods and chemical handling may possibly announce structural defects in graphene as mentioned above. There are numerous studies carried out taking place on the strength and elastic properties of defect-free graphene via first-principle, molecular-dynamics, and continuum mechanics simulations; however it is in its infancy stage regarding vacancy defect. In general vacancy defect can deteriorate the mechanical properties of graphene, thus why the author intended to study vacancy defect for modifying the failure behaviour of graphene sheet.

1.5 Objective of the Research

- Developing an atomistic model in molecular dynamics built environment toward studying its mechanical properties.
- Validation of interatomic potential for the modeling of single and multiple sheets of graphene.
- Reviewing the properties of pristine as well as defective graphene sheet;
- Exploring the effect of vacancy defects on single as well as multiple graphene sheets.
- To understand the transition in the failure mechanism of defective graphene sheets under the influence of non-bonded interactions in the bilayer sheets of graphene;
- Also studying non-bonded interactions simulation as well as stiffness of pristine graphene to quantify their impacts independently.
- On the road to examine the contemporary statistical methods for simulation of graphene sheets in presence of vacancy defect to comprehend the behaviour of the stress-strain relationship ;
- To study various areas of graphene applications for its leading, innovative and promising material;
- Characterizing to give detail description using molecular dynamics simulation regarding mechanical properties;
- Looking out the effect of mechanical properties at different vacancies, such as single vacancy, double vacancy and multiple vacancy.
- As a roadmap to guide the community towards the development of products based on graphene, related two dimensional (2d) crystals and crossbreed systems.

1.2 Thesis out line

The work that are designated in this thesis are all done on graphene using molecular dynamics simulation. Chapter 1 describes the theoretical background that is most relevant to the contents of this thesis. In chapter 2, I overviewed the basic concepts of molecular dynamics simulation and mathematical modelling used in this thesis. The contents focus on general concerns on mechanical properties of graphene. The main focus of the atomistic modelling in this thesis is on mechanical properties with vacancy defect and temperature. In chapter 3, we use to reveal molecular dynamics

simulation to validate Airebo potential using the massively parallelized modelling code LAMMPs software package (open software), and the atomic interactions are described by the CH.airebo potential in addition to necessary parameters. The amazing mechanical performance and properties of graphene based nanomaterials has attracted momentous research interests in current years so in chapter 4, we studied effect of vacancy defect. In chapter 5, we modelled the effect of non-bonded interactions on failure morphology of a defective graphene sheet.

CHAPTER 2

EXTENSIVE LITRATURE REVIEW OF EARLIER WORKS

Carbon is the powerful force after numerous technological revolutions in the 19th century, energy fabrication by burning carbon was essential to the industrial revolution in the 20th century, carbon-based plastics transformed the manufacturing industry in the 21st century, graphitic carbon or graphene might be a key constituent in a third technological uprising.

Over all, development of publications on graphene shown in Fig.4 below is increasing, without decreasing.

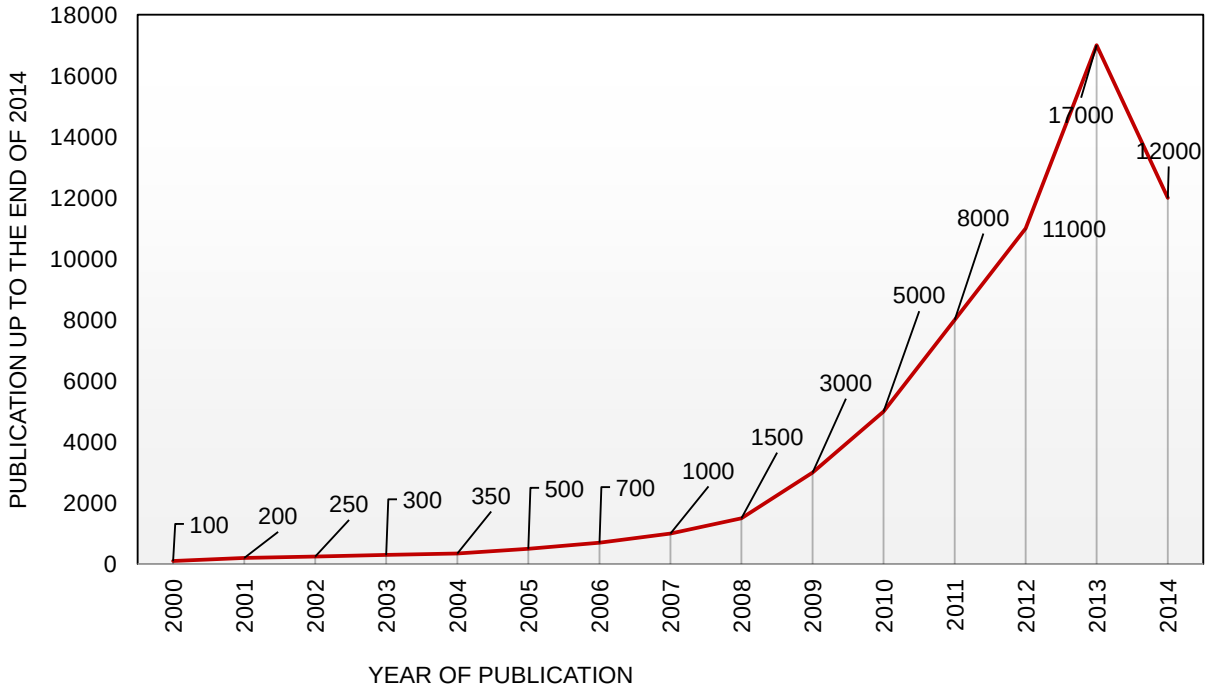

Figure 5. Publications on graphene from 2000-2014 (thus over all 18000 are expected at the end of 2014.publication on graphene earlier to 2000 were not outlined, Source: Web of science [34]

In general the study of the given below literature indicates the overview of graphene properties using molecular dynamics simulation by different researchers.

Rajasekeran G. Narayanan P and Avinash Parashar [2016][35]: They revealed that all-inclusive thoughtful of tough configuration property relations was necessary for developmental innovative for graphene based materials and nanocomposites for engineering applications.

Lee et al [2008][36]: Has experimentally explored the elastic properties of pure form of graphene is described towards the importance of high stiffness of (1 ± 0.10Tpa), which was in general measured the best value for young's modulus in graphene.

Frank et al [2007] [37] and Rasuli et al [2010][38]: Used the atomic force microscopy (AFM) based direct method aimed at finding the mechanical properties of thin atomic sheets of graphene and the same technique had also been used to estimate mechanical properties of few-layer thick graphene cantilever.

Suk et al [2010][39]: Used atomic force microscopic (AFM) techniques to determine mechanical properties of graphene and the results were validated with the finite element modelling. On the other hand numerical techniques had been achieved.

Shen et al [2014].[40]: For investigating result of, Shen et al and his scholar group employed molecular dynamics based simulations to study the effect of aspect ratio of graphene on its elastic properties of graphene. His group revealed that stiffness of graphene was, size and temperature dependent property that young's modulus decreases with increase in temperature and shear modulus was reported weakly dependent on the temperature.

Jiang et al [2009] [41]: Expected stiffness of graphene with respect to size of graphene and with high temperature. The scholars reported early in their molecular dynamics simulation that young's modulus of graphene usually shows increment with the increase in the size of the sheet.

Tsai and Tu [2010][42]: Recently in the year 2010, they performed a molecular dynamics based study on single sheet, and graphite fragments. They performed the molecular dynamics based simulation with two different types of ensembles, and they decided that modified NPT ensembles (Constant number of atoms, pressure and temperature of simulation box) for an upgraded accuracy on behalf of simulation to reveal the mechanical behavior of graphene, as compared to conventional NVT ensembles (number of atoms, volume of simulation box and temperature of simulation).

Ni et al [2010][43]: Studied the elastic properties of graphene using molecular dynamics simulations. He shown in his exploration work, elastic properties and fracture behavior of graphene was modelled regard to the direction of loading.

Parashar and Mertiny [2012, 2014].[44-45]: Same conclusion has also been made using numerical simulation to study the buckling stiffness of graphene. Additionally tensile loading via molecular dynamics modeling also achieved to simulate the double clamped twisting experimentation with the single layer of graphene. In their work, the relationship among the centerline deflection and accumulated forces has been derived from molecular dynamics in aggregation with the continuum theory.

Reddy et al. [2009, 2003, 2014, 2010, 2013, and 2012] [46, 47, 48, 49-56]: In their continuum based approach they studied the significance of energy minimization with respect to different elastic properties. Additionally to molecular dynamics simulation, finite division accounted by many scholars for estimating elastic behaviour of the sheet.

Y.Y Zhang et al [2011].[57]: He applied molecular dynamics simulations to reveal the bilayer graphene sheet tied by arbitrarily distributed sp3 inter-layer bonding. The inter-layer bonds in the bilayer graphene sheet remained created by showing increment moving two atoms with the same planar coordinates (one in upper layer and the other one in the lower layer) to the sp3 bond distance. Also, they used the bonding atomic interface in graphene sheet is defined by the reactive empirical bond order (REBO) potential. The aforementioned was found from the simulation outcomes that the occurrence of sp3 bonds can meaningfully boost the inter-layer contact and reducing the inter-layer space.

He et al [2014][58]: In their research work they have used the molecular dynamics based approach for simulating the consequence of STW tilting angle defect (STW1 and STW2) on the mechanical properties of graphene. Stated in their paper that by means of STW1 defective graphene, the stiffness in arm chair is lower than zig zag direction, whereas the contrary tendency reported with STW2 imperfections. More or less the scholars have also endeavored the road to model result of STW imperfection.

Canadija et al [59]: studied the outcome of atom disposition and concentrated toward bending behavior of graphene. This one decided commencing the finite element modelling having imperfections lying in the center of graphene has more impact on bending stress.

Jing and his research team [60]: studies the effect of STW and vacancy defect to see their effects on stiffness of graphene using molecular dynamics simulation.

Zhang and his group implemented molecular dynamics simulations for describing the outcome of single, di- and STW defects toward thermal conductivity of graphene [61].They also used defect density (which was well-clear as per the defected divided by the number of atoms in the pristine form); wherever each defect is preserved individually [62].

CHAPTER 3

MATHEMATICAL MODELLING TECHNIQUES FOR GRAPHENE

Experimental and mathematical approaches exist for illustrating different sorts of nanofillers Fig.5. Atomic force microscope (AFM), scanning electron microscope (SEM), transmission electron microscope (TEM), the X-ray diffraction (XRD), Raman spectroscopy,40 X-ray, photoelectron spectroscopy, and near edge X-ray absorption fine structure spectroscopy [63] were extensively recycled investigational procedures for characterizing nanofillers and nanocomposites.

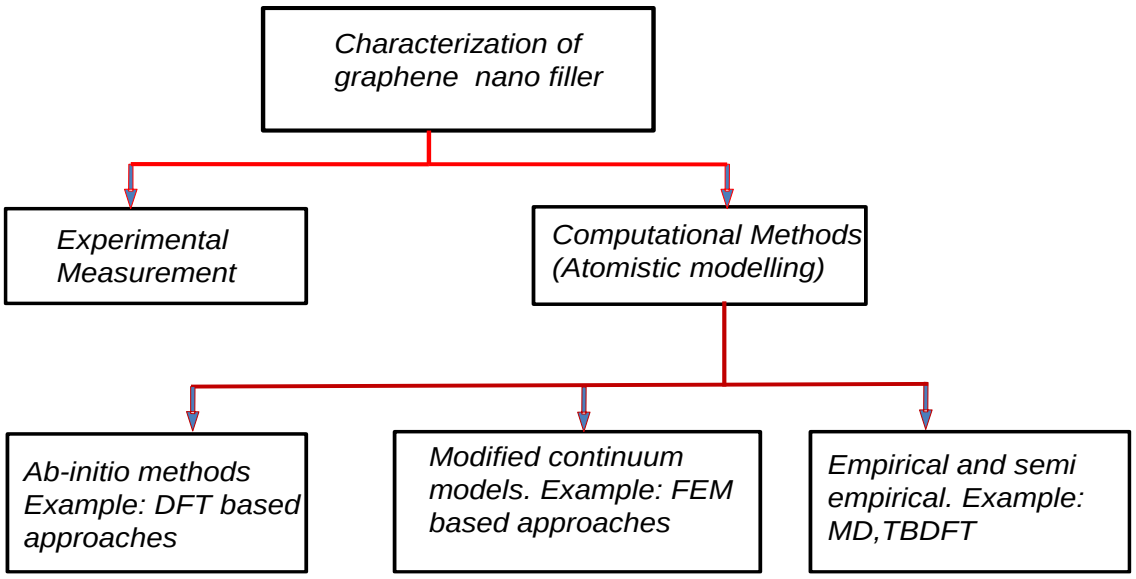

Figure 6. Description of nanofillers.

These dares inspire scholars to explore alternatives describing these nanofillers and nanocomposites. Because of remarkable progress in the numerical methods, numerical simulations are developing as a better alternative for describing these nanofillers and nanocomposites. Numerical models at t nanoscale classified in three subsections: Ab-initio (first principal) [64], semi-empirical, and modified continuum models.

3.1 Basic Concept of Molecular Dynamics Simulation

The origins of molecular dynamics are rooted in the atomism of classical time. In the former few decades, molecular dynamics simulations (MDs) have emerged as a very useful and significant tool to connect the predictions of theoretical models with experimental results, also to explain many of the microscopic mechanisms behind the measured properties. The expectation of materials' properties from their chemical alignment is crucial for the improvement of products at industrial level. Molecular dynamics simulations plays a vital role in the study of these materials, as they set up a very effective way not only for the computation of their macroscopic physical and chemical properties, but also for clarifying the atomistic mechanisms that determine these properties, thereby providing a link between the micro and macro levels.

Goal of atomistic simulations were demonstrating, examining, and accepting the motion of the each atom. Molecular dynamics computes the time reliant on performance of molecular system by integrating the equations of motion. Essential algorithm of molecular dynamics can be labeled in three steps:

(1) Initialization;

(2) Equilibration and,

(3) Calculation.

Molecular dynamics simulations may be considered as a technique of atom chasing. Molecular dynamics (MD) is a mechanics based computer simulation method in which the time evaluation is a set of interrelating atoms is trailed by integrating their equation of motion. There are three main computing methods for molecular close simulations;

- Mechanics technique,
- Molecular dynamics technique and,
- Monte Carlo technique.

In the technique of molecular mechanics, the properties of the system are calculated by considering first a collection of static microstructures. These microstructures are created by starting from an initial configuration where the particles are randomly arranged in the simulation

box. They are typically characterized by exceedingly large values of the potential energy because of the presence of atom-atom overlaps, thus the energy should be quickly minimized for these overlaps to be removed. The molecular dynamics method was built on second law equations of motion and elucidates standard comparisons of motion at individual phase. These equations are numerically integrated and the result of the integration yields the positions and velocity of individual particle or atom arrangement in course of time. In this way it is possible to study the time evolution of the simulated model system. And after system equilibration (at the prescribed temperature or pressure conditions), one can extract all the dynamical and structural properties of the system.

In the Monte Carlo method, thermodynamic average values are calculated via stochastic sampling of a very large number of configurations of the microscopic system. Monte Carlo techniques can efficiently exceed large energy barriers, thus allowing for the fast relaxation of the simulated system. But because the system is not allowed to evolve naturally in time, this technique cannot offer any information about the dynamical behavior of the system.

Molecular dynamics simulations follow the motion of all the atomic centers in the system by giving them as classical Newtonian particles (because the real systems of atoms by the side of fixed temperature are in persistent motion) and integrating the equations of motion:

$$f_i = m_i \frac{d^2}{dt^2} r_i \left(i = 1....N\right) \tag{1}$$

$$f_i = m_i \ddot{r} \tag{2}$$

Where; f_i force of atom, m_i mass of atom, $\ddot{r}$ acceleration of atom

$$f_i = -\frac{\partial E_i}{\partial r_i} \tag{3}$$

Where; ($i=1....N$) E_i, potential energy and r_i, position of atom

A system of atoms are allowed to move under these accelerations for a time period called time step. In stage two the new positions and velocities of the atoms are obtained using a numerical

integration method such as velocity Verlet method [65]. According the velocity Verlet method, also variation in r and v with Δt is graphical presented below;

$$v\left(t_o + \frac{\Delta t}{2}\right) = v(t_o) + \frac{[\vec{a}\,(t_o)\Delta t]}{2}, \tag{4}$$

$$r(t_o + \Delta t) = r(t_o) + v\left(t_o + \frac{\Delta t}{2}\right)\Delta t, \tag{5}$$

$$v(t_o + \Delta t) = v\left(t_o + \frac{\Delta t}{2}\right) + \vec{a}\,(t_o)\Delta t. \tag{6}$$

Where r,v and $\vec{a}$ are the position, velocity, and acceleration of an atom, respectively; to is the initial time; Δt is the time step. Variation in r and v with Δt is graphically presented in Fig. 6.

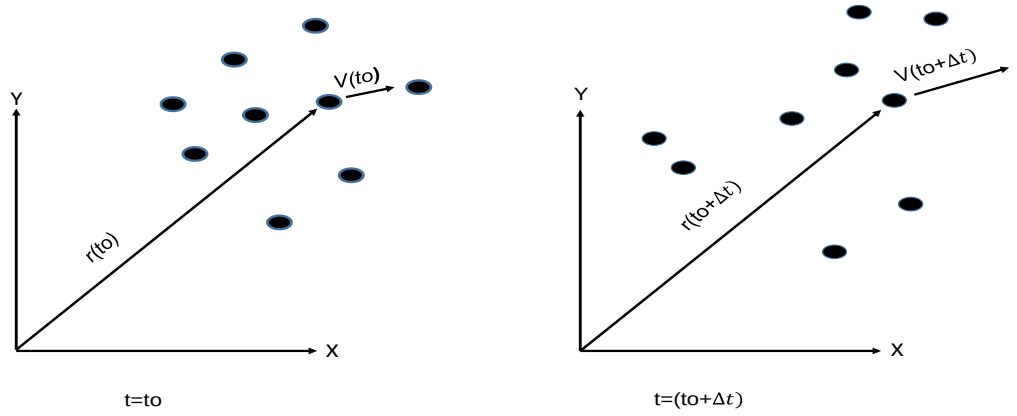

Figure 7. Change in position and velocities of atoms with time; where a system of atoms are allowed to move under these accelerations for a time period called time stage.

To obtain stress-strain (σ-ε) curve, using the following virial stress equation to estimate atomic stress of individual atoms during deformation:

$$\sigma_{ij}^{\alpha} = 1/v(\frac{1}{2}m^{\alpha}v_i^{\alpha}v_j^{\alpha} + \sum_{\beta=1,n} r_{\alpha\beta}^{j}\ f_{\alpha\beta}^{i})\,; \tag{7}$$

Here, i and j denote indices in Cartesian coordinates system; α and β are the atomic indices; m^{α} and v^{α} are mass and velocity of atom α; $r_{\alpha\beta}$ was the space between $\alpha\ and\ \beta$ atoms and V is the surrounding volume of atom α and the atomic capacity can be taken from the simulated graphene sheet with a width of 0.34nm [66]. In the same way, thermal conductivity (k) of the relaxed atomic arrangement expected using the below mathematical modelling:

$$K = \frac{J}{2A}\left(\frac{\partial T}{\partial x}\right) \tag{8}$$

$$J = \frac{\left[\sum N_{transfer}\ \left(m_h v_h^2 - m_c v_c^2\right)0.5\right]}{transfer} \tag{9}$$

Wherever $\frac{\partial T}{\partial x}$ was temperature deviation sideways the heat; A is cross- sectional area, J is the heat flux, transfer and $N_{transfer}$ are summation time and number of exchanges, respectively and c refer to hot and cold atoms, respectively.

In conclusion, stage three offers the useful outcome from the simulation. This may involve collection of statistical data (for the period modes of temperature and pressure, etc) or the writing of atomic trajectories for post giving out. Stiffness (E), breakage strength (σ_f), and rupture strain (ε_f) can be derived from the simulated σ-ε curves; the Young's modulus impact can be calculated as the initial slope of the σ-ε bends.

The strain energy stored in a graphene sheet at a particular strain is calculated by;

$$U_\varepsilon = E_\varepsilon - E_o \tag{10}$$

$$\varepsilon = \frac{L_f - L_o}{L_o} \tag{11}$$

Where; U_ε strain energy initial potential energy at strain ε, similarly E_o ,is the potential energy of the unstrained graphene sheet in demand to gain the stress-strain ($\sigma - \varepsilon$) relation of graphene ,a third order polynomial is fitted on the strain (ε) and the strain energy for each unit volume (U) data in the form of, $U = \frac{D\varepsilon^3}{3} + \frac{E\varepsilon^2}{2} + C\varepsilon + K$, where D is the third order elastic modulus, E is young's modulus ; C takes into account any residual stress in the graphene sheet and K gives full flexibility to the model. This one should be noted that young's modulus in this study is somewhat different from the conventional young's modulus which is defined as slope the linear part of ($\sigma - \varepsilon$) curve of graphene. However, the ($\sigma - \varepsilon$) curve of graphene is no-linear. Therefore; stiffness has

remained well-mentioned as the primary slope ($\sigma - \varepsilon$) curve stress (σ) is obtained by taking the first derivative of the strain energy in Eqn (above) with respect to ε as;

$$\sigma = \frac{\partial U}{\partial \varepsilon} = D\varepsilon^2 + E\varepsilon + C \tag{12}$$

$$Y = \frac{\left[\frac{\partial^2 U_\varepsilon}{\partial \varepsilon}\right]}{v} \tag{13}$$

A typical flowchart for an MD would look something like Fig.7. Amongst those steps the portion that, the greatest computational challenging is the force calculation. The effectiveness of an molecular dynamics simulation consequently rest on the performing force calculation as merely such as possible lacking negotiating the physical explanation.

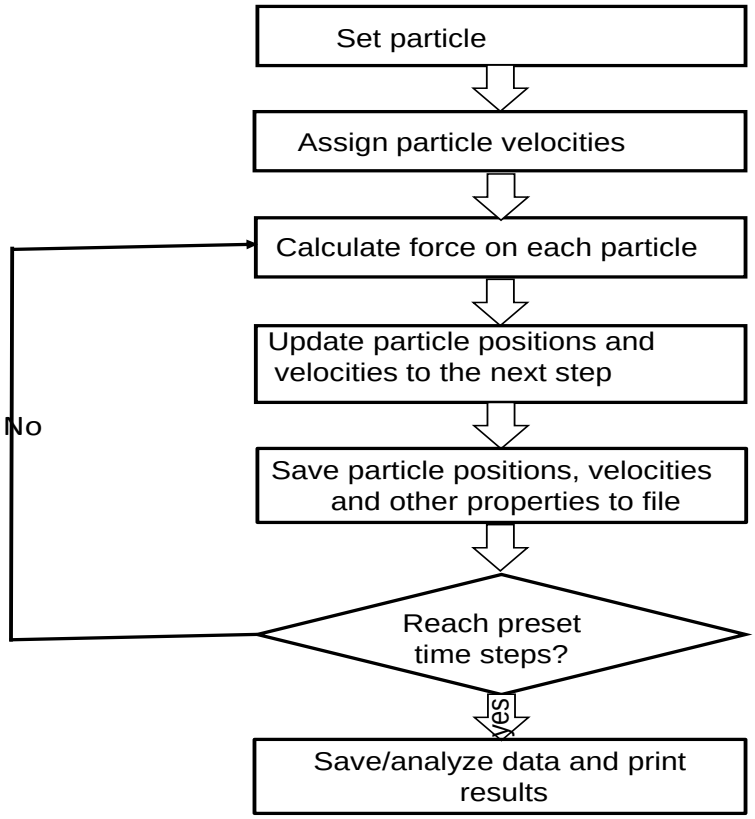

Figure 8.Stream graphic representation of molecular dynamics simulation.

3.2 Molecular Dynamics Ensembles

The main objective of MD simulation is to replicate a material's structure at atomic scale and predict macroscopic properties without directly depending on experiments. There are different types of ensemble averages used in MD simulation. Among these first three types of ensembles are widely used in MD simulations. This an ensemble is a group of all the promising states of a real system. The micro canonical statistical ensemble (NVE) describes an isolated system with a given number of particles N, a constant volume *V,* and a constant energy E. Molecular dynamics simulations obviously fit the NVE ensemble since energy is preserved by second law equations of motion. The canonical statistical ensemble (NVT) describes scheme with a given number of particles *N*, a constant volume *V*, and a constant temperature *T*. The isothermal-isobaric statistical ensemble describes a system with a given number of particles *N*, a constant pressure *P* and a constant temperature *T*. It is the most common ensemble used in molecular simulations, because it reproduces the behavior of a material in real conditions of pressure and temperature. The micro canonical N, V, and E (NVE) ensembles, the canonical (NVT) ensembles, and the isothermal-isobaric (NPT) ensemble are frequently used in MD simulations. The contractions N, V, E, T, and P stand for the number of atoms, volume, energy, temperature, and pressure of the system, respectively and these quantities are kept constant during the simulation. The goal of molecular dynamics simulations is to deliver evidence about the physical properties of a macroscopic system. A difficulty to overcome in these calculations was, that they are computationally time taking, limiting in most cases the size of the simulated system to only a few thousands of particles.

3.3. Integration of the motion equations

The rules of motion are termed by ordinary differential equations, where the relevant functions, such as position or velocity depends only on time in classical particle dynamics.

$$x(t + \Delta t) = x(t) + \dot{x}\, \Delta t.. \tag{14}$$

3. 4 Verlet algorithms

The Verlet algorithms are easy, precise and, as we will see below, time reversible, which explains why they are widely used in MD simulations. Verlet's algorithm is derived by the Taylor expansion of the position. Original form of the Verlet equations is gotten by utilizing a Taylor expansion at times t -dt and t +dt:

$$r(t+dt) = r(t) + v(t)dt + \frac{r(t)dt^2}{2} + \frac{\dddot{r}(t)dt^3}{6} + \cdots. \tag{15}$$

$$r(t-dt) = r(t) - v(t)dt + \frac{\ddot{r}(t)dt^2}{2} - \frac{\dddot{r}(t)dt^3}{6} + \cdots \tag{16}$$

Summing the two equations gives:

$$r(t+dt) = 2r(t) - r(t-dt) + \frac{\ddot{r}(t)dt^2}{2} + \cdots \tag{17}$$

With $\ddot{r}(t)$ calculated from the forces at the current positions. The calculation of the velocities is obtained by subtracting eq. (16) from eq. (15): Verlet algorithm needs two steps to grasp the future location from the current and previous location info. Initialization of algorithm can thus be done by using the initial space and velocity information and applying the Euler method as given in Equation (15).The preliminary velocity supply is given according to statistical mechanical requirements of the system. Verlet algorithm does not use velocity information afterwards. Velocity at time t, can be designed using the central difference technique, which stated as equation below;

$$v(t) = \frac{[x(t+\Delta t) - x(t-\Delta t)]}{2\Delta t} \tag{18}$$

From a mathematical point of view, the problem of the potential energy minimization belongs to the general category of optimization problems. The main goal of the optimization problems is to choose appropriate values for the variables $x1, x2, x3, \ldots, xN$ so as to optimize (minimize or maximize) a scalar function $f(x1, x\,2\,x3, \ldots, xN)$. In molecular simulation problems, this function is the potential energy of the system $U(rN)$; its optimization corresponds to the minimization of its value. So, the target is to find the optimal values of the particle positions in the system so that the total potential energy reaches a minimum.

3.5 Interatomic Potentials for Graphene

Potential field is one of the best mathematical account of the potential energy of a system interrelating particles. The key objective of this inter atomic potential field is to give mathematical description terminologies by approximating the energy landscape of a large atomic system. Various researchers concluded that all achievement of any atomistic simulation is relays on the success of interatomic potential which is active for simulating the bounded and non-bounded interaction b/n the atoms [67]. A lot of interatomic potentials or force fields have been advanced, ranging via different levels of precision and densely however the simplest form of atom-atom interaction is pair potential; the potential energy of which only rest on the space among two atoms. Total energy of the scheme given by adding the energy of all atomic links ended all a particles which is happening to the scheme. The overall arrangement of potential energy description is;

$$U_{tot} = \frac{1}{2} \sum_{\alpha=\beta=1}^{N} \sum_{\beta=1}^{N} \varphi \ (r_{\alpha\beta}) \tag{19}$$

Where $r_{\alpha\beta}$ is the distance between particles α and β , $\phi(r_{\alpha\beta})$ is the potential energy between particles α and β .

The general form of a potential field can be expressed as;

$$E_{tot} = E_{covalent} + E_{non-covalent} \tag{20}$$

Where; E_{tot} total energy, $E_{covalent}$ covalent energy and $E_{non-covalent}$, non-covalent energy

$$E_{cov} = E_{bond} + E_{angle} + E_{dhedral} + E_{out\ of\ plane} \tag{21}$$

$$E_{non-cov} = E_{electrostatic} + E_{vanderwals} \tag{22}$$

Scholars had used Morse potential field; reactive empirical bond order (REBO) potential field and adaptive intermolecular reactive empirical bond order (AIREBO) potential field for simulation of graphene and carbon nano tubes [68]. AIREBO potential was an improved version of REBO potential, which contains an element for non-bonded interfaces and one more component for four body torsional interfaces. AIREBO [39] and [69]. Potential field is an extension of the commonly used REBO potential field; where AIREBO addresses some of the short coming in the REBO potential. Absence of the non-bonded interaction in REBO potential makes its poorly suitable for

systems with significant intermolecular interactions such as graphite [70]. AIREBO potential contains three sub- section potentials. They are;

1. Reactive empirical bond order (REBO),
2. Lennard-Jones and;
3. Torsional potentials;

Wherever the REBO potential provides the energy stored in particle links; the Lennard-Jones potential contemplates the non-bonded interfaces among the atoms, and the torsional potential captures the energy from torsional interactions amongst particles. AIREBO potential consists of three parts that can be expressed mathematically as follow,

$$E^{AIREBO} = \frac{1}{2}\sum_i \sum_{i\neq} \left[E_{ij}^{REBO} + E_{ij}^{LJ} + \sum_{k\neq i,j} \sum_{l\neq i,j,k} E_{ijk}^{ltors} \right], \quad (23)$$

From this wherever i,j,k and l states to each particle, E is the sum of potential energy, E_{ij}^{LJ} is the an element which representing non-bonded Lennard Jones potential, E_{ijk}^{ltors} stand for the four – body torsional term in AIREBO, and E_{ij}^{REBO} is the REBO potential . REBO potential be made up of two mathematical elements; which consists attractive and repulsive terms as described below.

$$E_{ij}^{REBO} = f(r_{ij})\left(E_{ij}^{Repulsive} + b_{ij}\ E_{ij}^{Attractive}\right), \quad (24)$$

Where b_{ij} is the bond order which regulates the bond strength, f (r_{ij}) is the cutoff function limits the bonded interaction among to the nearest neighboring atoms lying within the cut off distance.

3.6 Cut-Off Radius

On the way to exist the inter-atomic potential energy function must be constructed in such way that the energy involvement allocated to a given atom is only affected by atoms within a specified distance which is called cut-off radius denoted by (r_{cut}). A lesser value for cut-off radius improves the computational efficiency, also on the other pointer it diminishes the exactness of the simulations, hence cut off radius is frequently explained in a way that exactness of the calculations

will not be affected. To investigate the effect of defects in graphene, Wu et al. [71] used a value of 1.92$\dot{A}$, while Jhon et al. [71] used the value of 2.0$\dot{A}$ as the c-c bond cutoff radius in order to avoid unphysical results before the bond breaking.

To study the consequence of cut-off radius on the flexible strength of graphene, different cut off radius used in different research works is compiled in Fig.8. [72]. However, experiments [73] and ab initio calculations [74] have given smooth nonlinear stress-strain curve without any strain hardening. It can be concluded from the trend shown below in Figure 4; that flexible strong point of graphene is continuously slow down through an increment in cut off radius from 1.75–1.92 $\dot{A}$ [75].

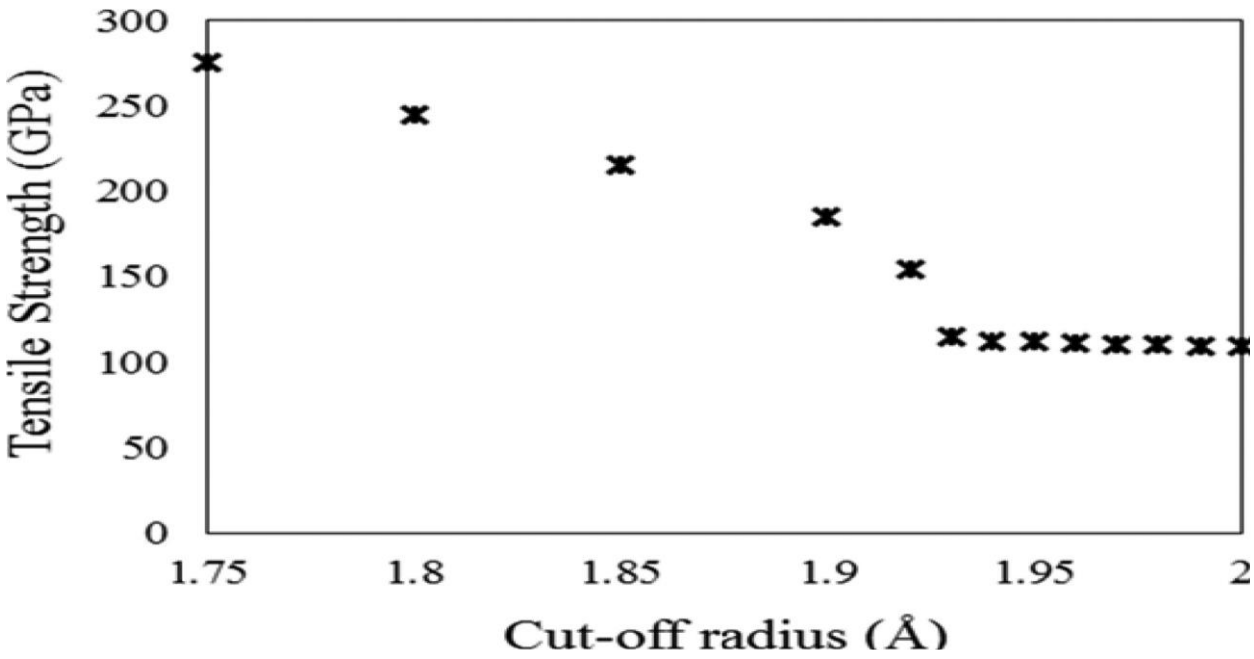

Figure 9. Association among modelled tensile strength and C-C bond cut-off radius (adapted He et al.75).

In order to further investigate the effect of cut-off function on the fracture simulations and also to find an appropriate cut-off radius for the crack simulations of graphene, potential energy of C-C bond between atoms 1 and 2 in Fig.9 is arithmetically gained with the increment of bond length r; where the relative positions of other atoms were kept unchanged.

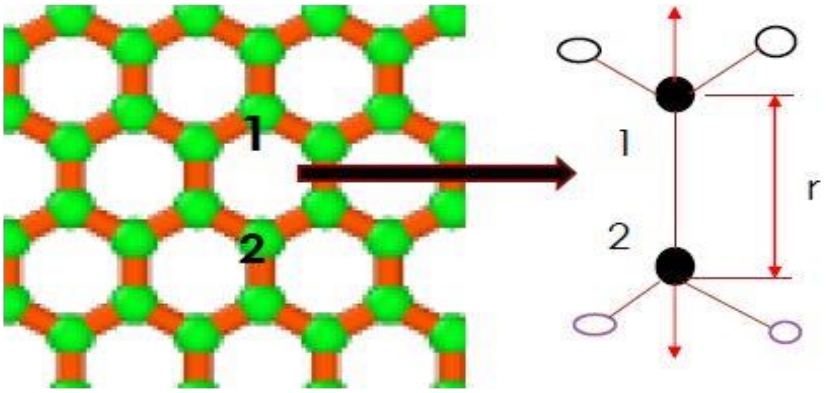

Figure 10. The system used to investigate the cut-off effect. The arrows indicates the straining direction and r is the initial bond length.

CHAPTER 4

MOLECULAR DYNAMICS SIMULATION TO VALIDATE AIREBO POTENTIAL

On the way to simulation of graphene, molecular dynamics simulation (MDs) was built that contains 800 carbon particles by regular size of, Lx =49.2Å and Ly= 42.6Å or (4.92nm by 4.26nm) shown in Fig .10. All the parameters mentioned in above are predefined parameters in MD simulation. However some MDs parameters such as time step, strain rate, and boundary conditions are user defined parameters. Selection of these parameter has an influence on the MD simulation. The size of monolayer graphene sheet we considered was $49.2\dot{A}$ x $42.6\dot{A}$ as mentioned above given dimension; were achieved via the modelling programmed LAMMPs software package (open software), besides the atomic interfaces are described by the CH.airebo potential, where cutoff parameter AIREBO was modified as 2.0 to avoid nonphysical high force. In our case periodic boundary condition was applied in all directions. Larger time steps increase the computational effectiveness and lesser time steps may upturn the exactness of the simulation. Therefore, the time step controls the trade-off among exactness and computational effectiveness in a MD simulations; so that if a time step is selected too large, the system might become unstable. However, scholars ought to use time steps from 0.1 fs to 1 fs to simulate uniaxial tensile tests of graphene [77, 78]. Actually, mostly they have used AIREBO potential field applied in LAMMPS MD simulator for the simulations. Therefore; it is interesting to investigate the effect of time step on the simulation of the uniaxial tensile test of graphene. In MD simulations the other parameter is, a tensile test which performed by applying strain to the nanostructure at persistent strain rate. Scholars had establish, that the failure point of graphene be contingent on the strain rate [79-80]. On the lower strain rates, the system have more time to relax and reach equilibrium state; and the outcomes would be more exact. Practical strain rates, used in this investigation is $5x10^{9}\ divided\ by\ 1x10^{12}\ or\ 5x10^{-3}\frac{1}{s}$, which is possible in this simulation due to effective computational efficiency. Scholars had used several strain rates starting from 0.0005 pico per seconds to 0.01 pico per second [81]. In order to investigate the effect of strain rate on the failure

point of graphene, a set of MD simulations were performed on a graphene sheet of size 5 nm x 5 nm under the strain rates of 0.01 pico per seconds, 0.001 pico per seconds, and 0.0001 pico per seconds. Therefore, in our case, in order to become computationally feasible, strain rate of the order of 5 $*10^9$ ($5x10^{-3}\frac{1}{s}$), is generally used in MD simulations. The other parameter is time combination using Nose-Hoover with non-Hamiltonian equations of motion considered to produce space plus velocities tasted from the canonical (NVT), isothermal-isobaric (NPT), and isenthalpic (NPH) ensembles. Molecular dynamics simulation takes place in a simulation box where the size of this simulation box is determined by boundary conditions. The most commonly used boundary condition is the periodic boundary condition since it can represent an infinite number of atoms by performing the simulation in only a single unit cell. In general the tensile load was applied to the graphene sheet alongside to both armchair and zigzag directions. The model was accompanied at a strain rate of 0.005 $ps^{-1}$and at a time step of 0.001 ps. The model was firstly simulated to a minimum energy state with the conjugate gradient energy minimization. Then, Nose–Hoover thermostat [82, 83] were active to equilibrate the graphene sheet at a certain temperature by means of periodic boundary conditions. Recalling that adaptive intermolecular reactive bond order (AIREBO) potential was [84] applied in the software package LAMMPS [85], to simulate covalent bond formation and bond breaking.

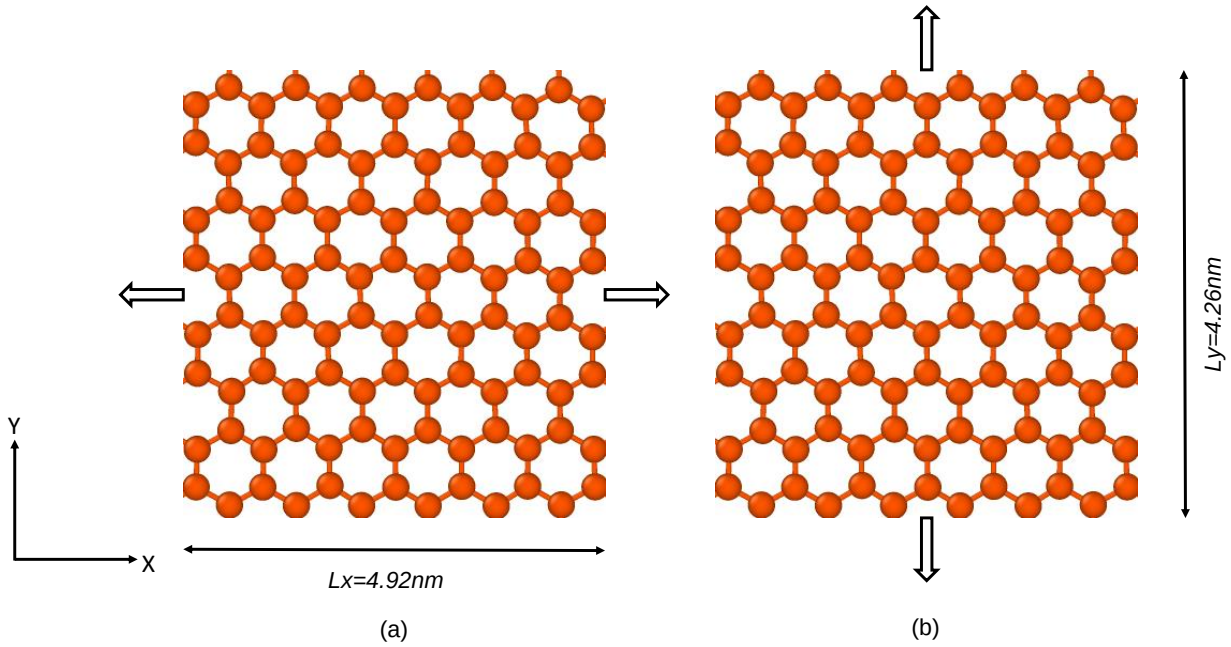

Figure 11. Model of graphene sheet: same tension alongside (a) zig-zag way and (b) armchair way.

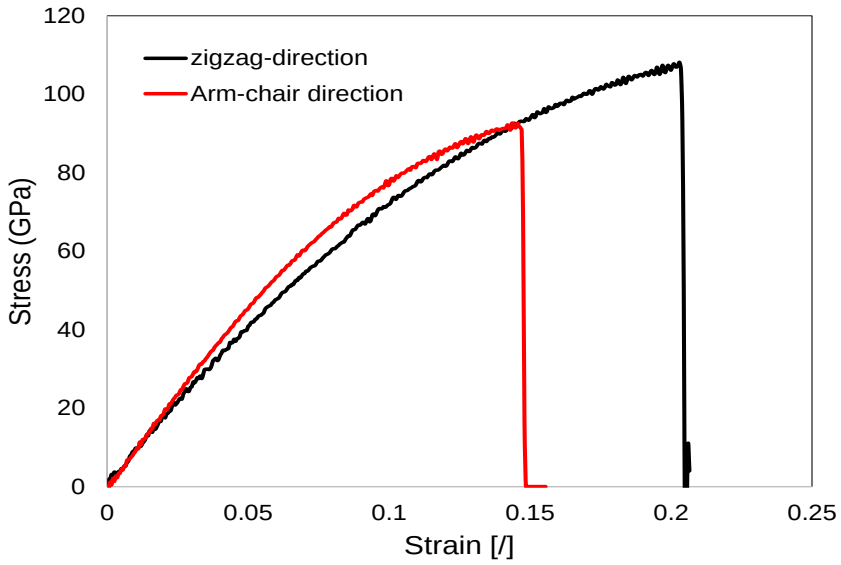

Figure 12.On the way to confirm mathematical method, the fracture strength of a pristine graphene sheet was initially calculated. Stress-strain bends of pristine graphene sheet under same tension along zigzag way (black colour) and armchair way (red colour) at 300K.

In the direction of validating the mathematical method, the rupture stress of pure graphene sheet was initially designed. Consequence of minimal stress-strain bend next to the temperature of 300 K, subjected to tension load alongside both armchair and zigzag directions shown above Fig.11,

was revealed, that fracture stress beside the armchair and zigzag way is calculated as 91 and 106 GPa, separately. In Cauchy stress; the rupture stiffness was 100GPa and 126 GPa and the rupture strain is 0.13 and 0.22 correspondingly. These results were promise new examination, i.e., $\sigma_f \approx 130$ GPa and $\epsilon_f \approx 0{:}25$ [86] as well as previous numerical simulation [87], verifying dynamism and exactness of our mathematical approach. One of the most important output from MD simulation was the potential energy of the graphene sheet at the time of relaxation period. Deviation of potential energy of the sheet with time is shown in Fig.12. Potential energy is almost constant during the relaxation period was (up to 5ps) then start to increase with the applied strain with a strain rate of 0.005 ps-1.

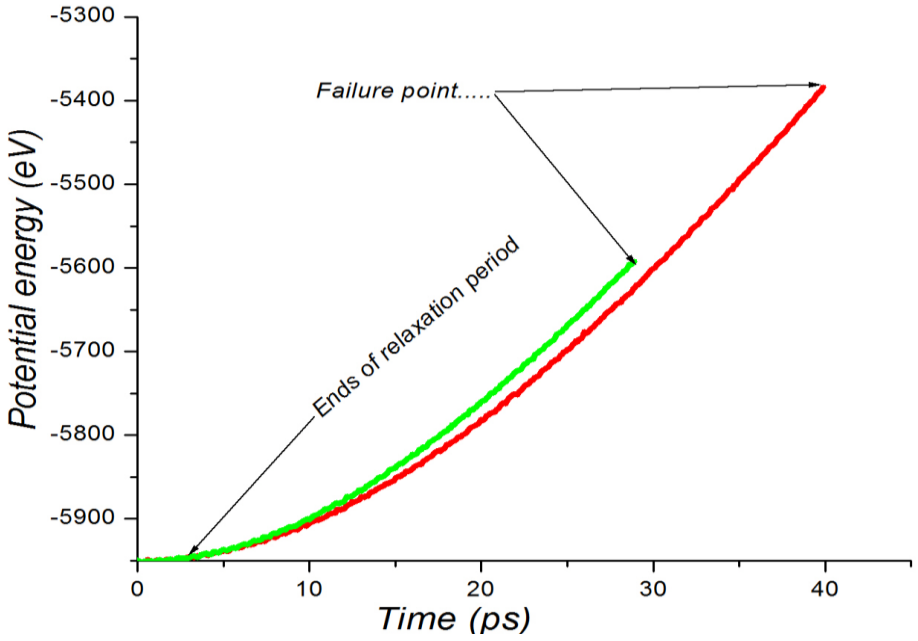

Figure 13. Change in the potential energy with time.

Also graphene can be subjected to higher temperature at production stage as well as when graphene based devices operate at higher temperature. As we discussed above Chemical vapor deposition (CVD) is one of the most commonly used methods of graphene manufacture; that products graphene at a temperature of around 800 K. Therefore, understanding the temperature behavior of graphene helps to fabricate best excellence graphene founded devices. Studying the effect of high temperature on mechanical properties of a substantial armchair and zigzag is presented.

In the temperature range of 200K, 300K and 450K, the breakage stress with vacancy was evaluated subjected to load; along armchair and zigzag way. Modelling was held at temperature of 200K, 300K AND 450K as shown in Fig.13. (a), and (b) Shows the fracture strength σ_f for the graphene sheets without defect at temperatures of 200 K, 300 K, and 450 K.

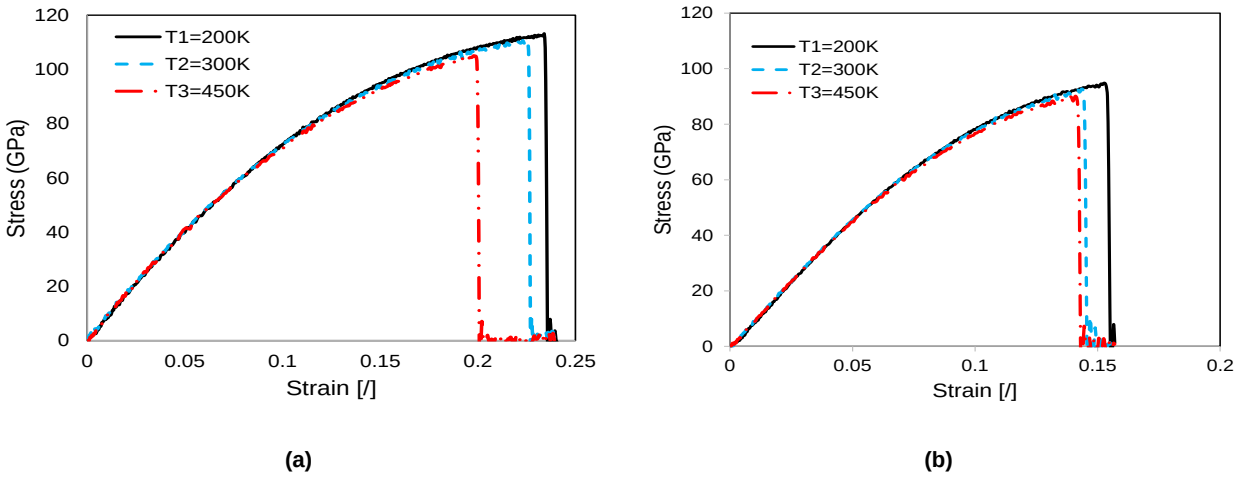

Figure 14. Stress versus strain curves; (a) Zigzag direction graphene sheets at different temperatures, (b) Armchair direction graphene sheets at different temperatures.

This section at all reviewed the concept behind MD simulations. A set of MD simulations were done in order to examine/study the result of some MD parameters are, potential field, strain rate, and time step. Non-physical characterization in the stress-strain curve was convinced by default cut-off function of REBO potential that can be removed by changing cut-off radii to $2\dot{A}$. Strain rate does not mark Young's modulus, however the higher strain rate outcome in a greater decisive stress and strains. Time step does not have an impact on the stress-strain graph. The intermolecular interfaces and torsional interactions of AIREBO potential do not affect the stress-strain curve.

CHAPTER 5

RESULTS AND DISCUSSIONS

The incredible mechanical character and properties of graphene-centered nanomaterial's fascinated momentous exploration interests currently; outstanding to their promising forecasts in multipurpose subdivisions for example micromechanics, microelectronics, and thermal applications. It's known to have ultra-high stiffness and strength, yet a wide scatter have been observed towards mechanical properties. Pure graphene sheet were reported high stiffness resembling graphite (~1.0 TPa), in addition to its greater strength (90GPa~100 GPa on behalf of tensile load and 50GPa~60 GPa used for shear load) that it arises from a combination of high stiffness, rare elasticity and resistance to rupture. Also the imperfections of material production procedure, device or composite fabrication, chemical treatment, particle irradiation and mechanical loading can all encourage defects. In this thesis paper consequence of a lack imperfection on strength of graphene will be held because, if an atom removed from the lattice, its neighbours will become unstable because of their sp^2 bonds are not saturated [88].

5.1 Vacancy Defects

Lack of atoms from the lattice of graphene is frequently labelled as vacancy defects, which can be further sub classified as; single, di- and multi- vacancy weaknesses are centered on number of atoms absent from the lattice. Vacancy defects can reduce the strength of graphene by around 50%. This section presents a detailed study of the result imperfection weaknesses along armchair and zigzag way. Molecular dynamics simulations presented in this section have been conducted with PBCs where the edges of the graphene sheets have not any impact on the simulation outcomes. Nevertheless, the finiteness of sheet could have an effect on the MD simulations with fracture. In direction to explore the consequence of finiteness, a set of armchair sheets of various sizes were exposed to the uniaxial tensile test at 300 K.

- Deficiency one carbon atom from the graphene frame proceeds a mono-vacancy;
- The di-vacancy can happen by the elimination of two carbon particle.
- The deletion of two or more carbon atoms can takes to a multi vacancy defect which is larger and have a more complex defect configuration.

The same conclusion has been made in this thesis paper, that stiffness of graphene with mono- is lower as compared to di-vacancy imperfections with same number of lost atoms.

5.2 Modelling and Methodology

The dimension of the graphene monolayer sheet was measured as $49.2\dot{A} \; x \; 42.6\,\dot{A}$. The initial vacancy imperfections were arbitrarily dispersed on sheet plane affording to a prearranged defect ratio, which is defined as the ratio of misplacing atoms against total atoms in the complete pure sheet. The engineering strain rate was $0.005\ ps^{-1}$ besides the strain rise was applied in each 50000 time periods. The mechanical test where implemented to develop the stress versus strain curve relations and the associated parameters, namely stress-strain and the value of simulated graphene in zigzag and arm-chair directions are shown below in table 2 &3.

Table 2.Mechanical properties: Stiffness of pristine and imperfection investigated.

Imperfection types	Methods adapted	Tensile strength (GPa)	Young's modulus (TPa)
Pristine graphene (Arm-chair direction)	Molecular dynamics	91	0.89
Pristine graphene (Zigzag direction)	Molecular dynamics	106	0.91
Single Vacancy	Molecular dynamics	86	0.8
Double Vacancy	Molecular dynamics	76	0.74
randomly distributed vacancy	Molecular dynamics	64	0.58

Table 3. Fracture Properties of defect free and defective graphene sheet investigated.

Types of Defects	Methods Adopted	Fracture Strength (GPa)	Fracture Strain
Pristine graphene	Molecular dynamics	106	20%
SV defects	Molecular dynamics	80.1	12.8%
Dv defects	Molecular dynamics	57.12	16.95%

Initially we analyzed the structural distortions of graphene sheets with defects. The defective graphene sheets are created from pure graphene films by eliminating atoms. Once structural relaxation at zero temperature; the atoms on the sheet have a tendency to re-arrange their local places to set of scale the spatial stress. Stress-strain relations exhibit numerous stress crests besides total multiple breakage performance as shown in Fig.14.

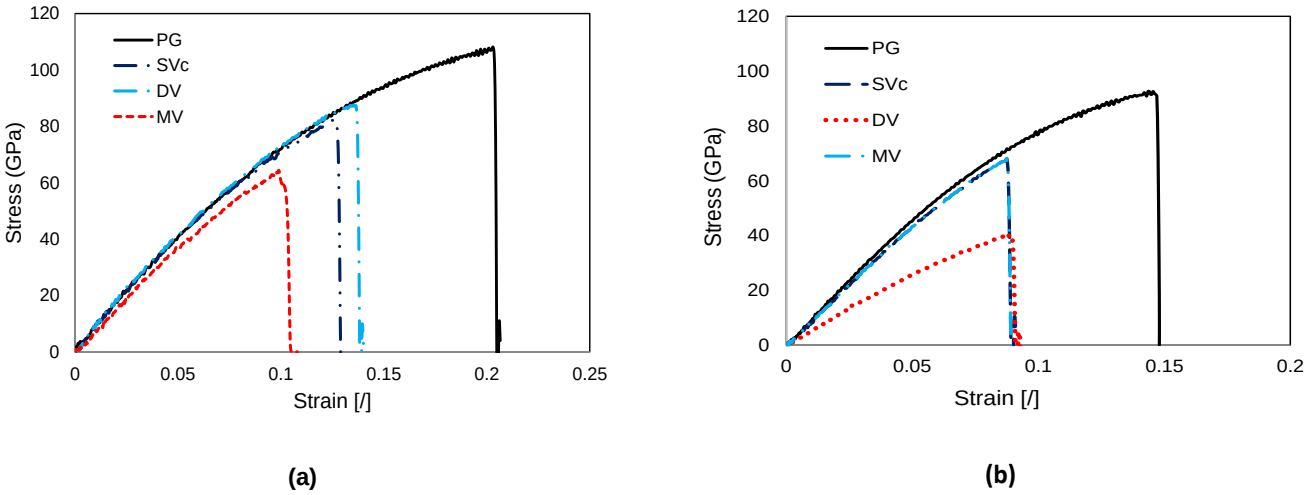

Figure 15 Stress-strain bends of unperfected (a) zigzag (b) armchair direction; where PG (pristine graphene), SVc (single concentrated vacancy), DV (di-vacancy), MV (multi-vacancy).

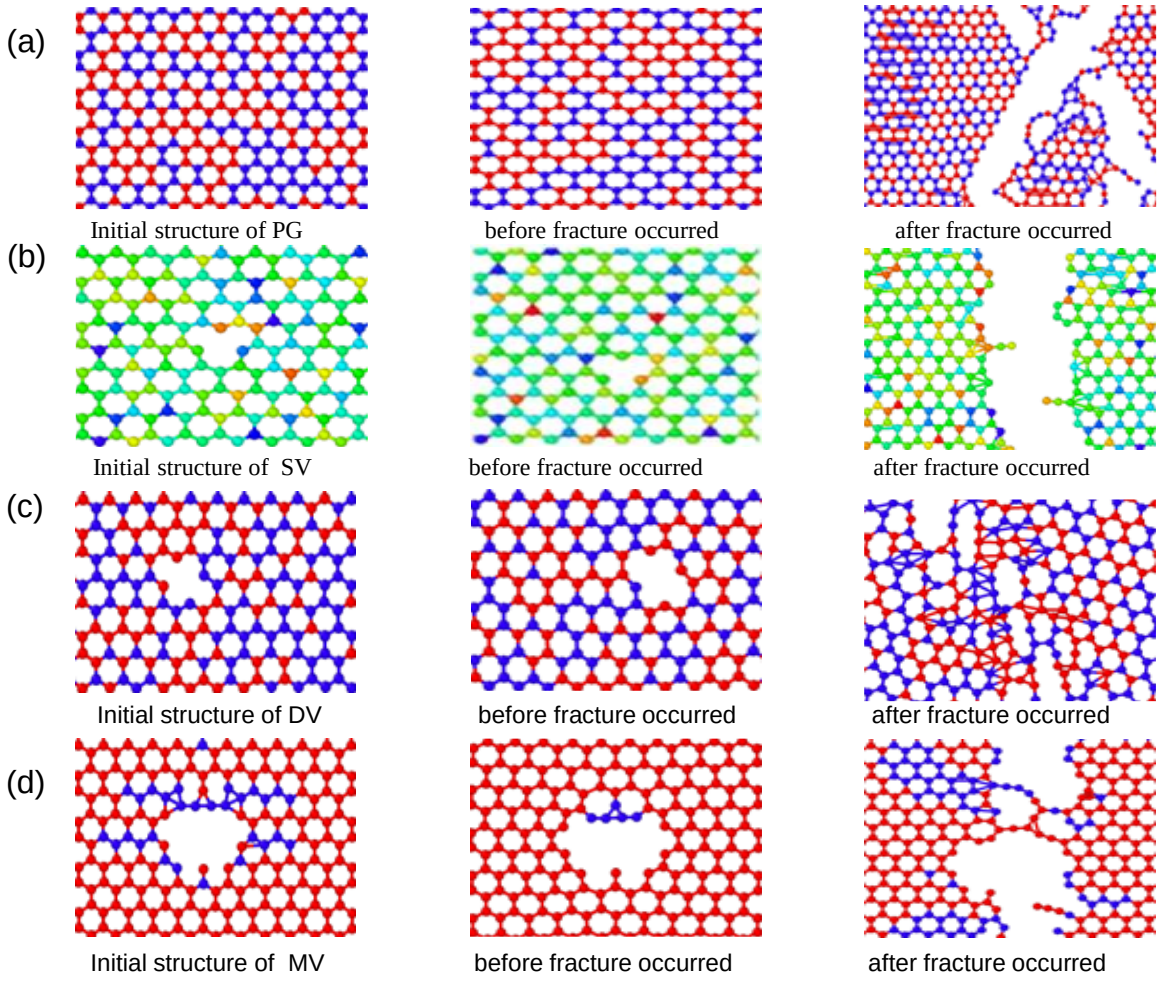

Figure 16. Steps of breakage development in graphene covering cluster-type vacancy, (a) pure graphene, (b) mono-vacancy, (c) di-vacancy, (d) multi- vacancy. Here, PG, SV, DV and MV refers to pristine graphene, single vacancy, di-vacancy and multi-vacancy at initial structure.

The stress -straining bends with a cluster-type vacancy at 300k were presented below Fig.16.

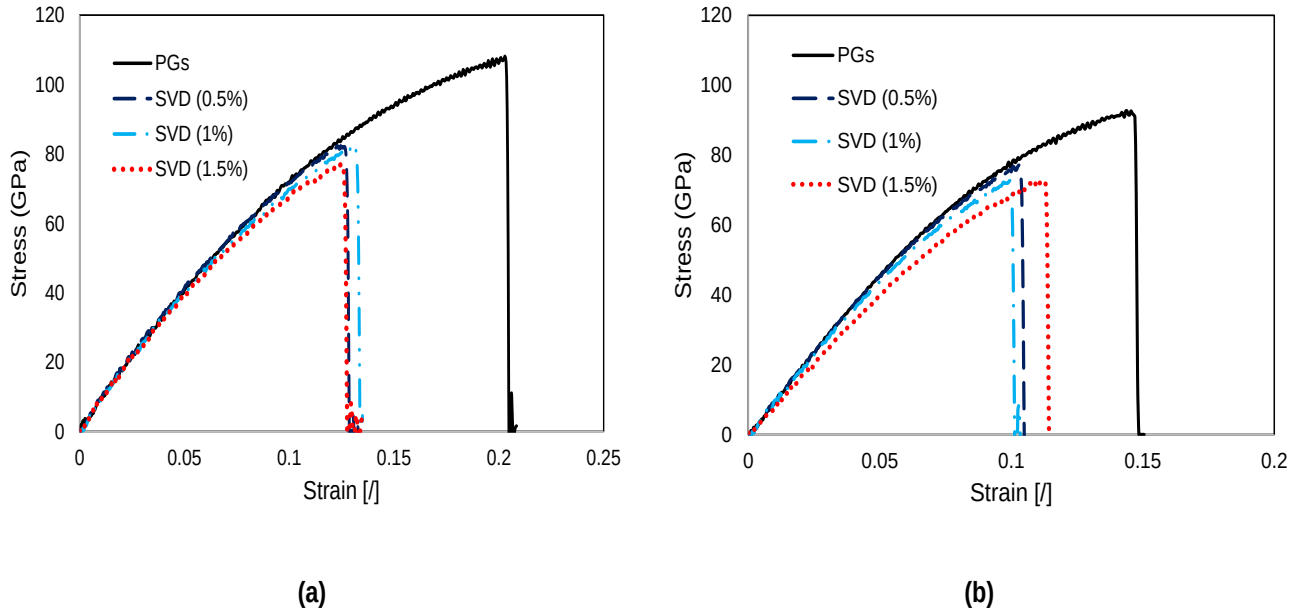

Figure 17. Stress-strain bends containing group type vacancy under tensile deformations along (a) Zigzag (b) armchair direction. Results of pristine graphene sheets with low and high defect ratio was revealed using single vacancy distributed, (a) pristine graphene (PG) (0%), single vacancy distributed (SVD) (0.5%), (1%) and (1.5%) (b) Pristine graphene (PG) (0%), single vacancy distributed (SVD) (0.5%), (1%) and (1.5%).

The material becomes less strong on the other hand extra ductile, decreasing ultimate strengths and inflating fracture strains. Slight drops in stress-strain relations are supposed to originate from geometric redisposition on the graphene sheet (to dissipate the accumulated loads or energy).The effect of multiple defects on strength depends on the residual dangling bonds induced by vacancy defects, which weakens the bond structure significantly and enhances the mobility of carbon atoms strongly. The multiple stress peaks pose difficulty in determining the fracture point. However, the entire energy of scheme increases with incremental strain preceding last fail. Therefore, we define fracture point as the highest energy point. This phenomenon also directs large strain, even if strong point remains almost unchanged, the potential energy of the system can still be increased.

5.3 Mechanical properties under tensile deformations

Failure morphology of the graphene with uniformly distributed vacancies during strain failure vs vacancy defect ratio were displayed in Fig.17. a very instance, concentrated stress occurred near unperfected; at that moment breakages happens opening from were vacancy defect started then growth in the direction of nearby defects where fracture starts randomly from the defect of vacancies exist. We now turn to analyze the mechanical properties at failure point for defective graphene. It should be noted that the ultimate strength is the maximum stress in the stress-strain curves, while the fracture strain is determined from the spontaneous large drop of the total energy increment curves. Without defect the ultimate tensile strength is 91GPa and 106 GPa intended for armchair and zigzag graphene, separately.

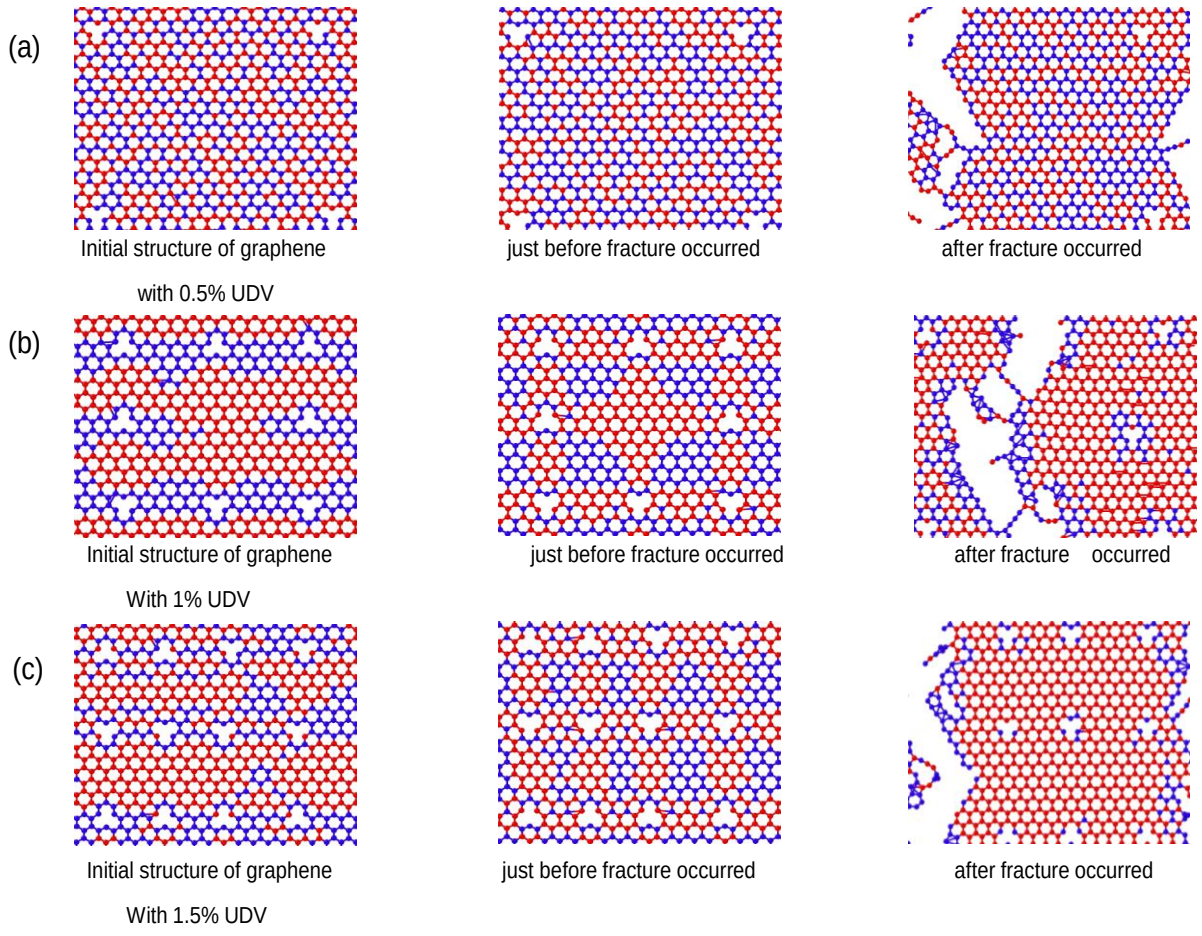

Figure 18.Steps of breakage development in graphene having evenly concentrated vacancies. The vacancy defect ratio was (a) 0.5%, (b) 1%, (c) 1.5%, where, UDV refers to uniformly distributed vacancy defect ratios.

On behalf of through evenly concentrated defects, correlation among stress, strain besides defects are revealed below Fig.18 & 19. Obviously the stress decreases with the increase in vacancy defect and the strain failure decreases with increase vacancy defect. On or after this we decided that in contrast, stiffness to some extent drops by rise in vacancy Fig. 19 defect; because lack of an atom implies vacancy defect that graphene is more sensitive to vacancy where carbon bond breakage is happen at the time.

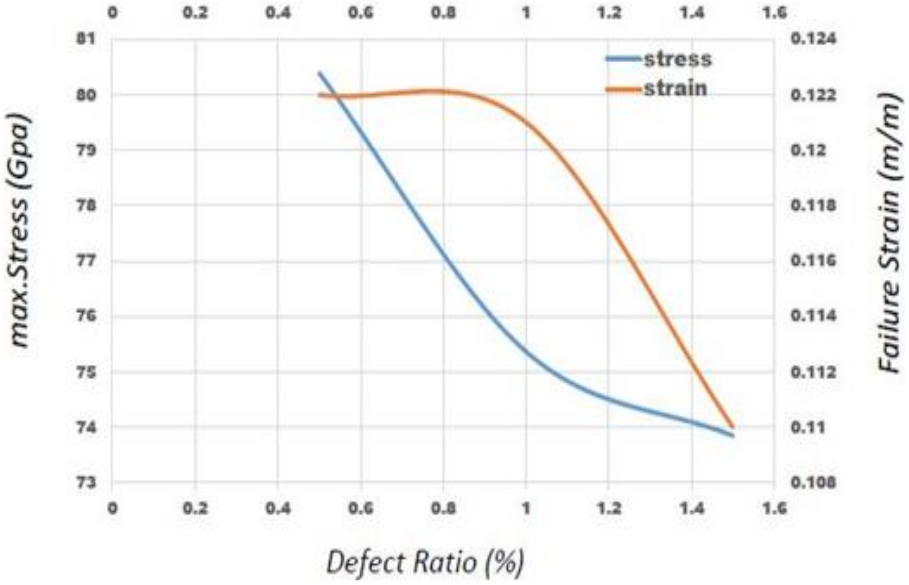

Figure 19. Breakage strong point of unperfected graphene sheet on stress and strain against the number of vacancy defect ratio in Zigzag direction. Both lines remain the outcomes of quantized fracture mechanics (QFM).

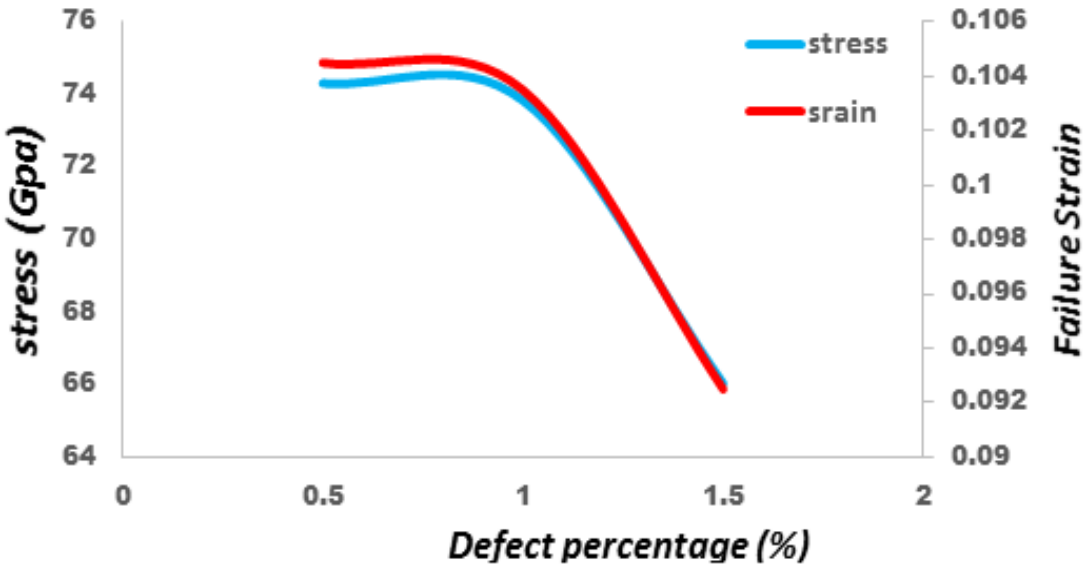

Figure 20. Breakage strong point of unperfected graphene sheet on stress and strain against the number of vacancy defect ratio in Arm-chair direction direction. Both lines remain the outcomes of quantized fracture mechanics (QFM).

CHAPTER 6

EFFECT OF NON-BONDED INTERACTIONS ON FAILURE MORPHOLOGY OF A DEFECTIVE GRAPHENE SHEET

6.1 Introduction

Graphene is a two dimensional planar arrangement of carbon atoms. Sp2 hybridized hexagonal arrangement of carbon atoms in the structure of graphene is attributed for its exceptionally high mechanical, thermal and electrical properties [89]. Remarkable mechanical properties of graphene-based nanomaterial has concerned crucial research interest in recent years, due to their promising forecasts in adaptable branches such as micromechanics [90], microelectronics [91], and thermal [92] applications. In addition to these nanotechnologies, graphene is also listed among the top potential nanofillers for developing nanocomposites with improved mechanical properties, thermal and electrical conductivities [93-94]. Diversified field of applications, exceptional properties have motivated researchers for exploring new production techniques for developing graphene. Graphene can be produced by means of chemical vapor deposition (CVD) [95], mechanical exfoliation [96], chemical reduction of graphene oxide sheets [97], etc. On the other hand, both material production methods and chemical treatment may introduce structural defects in graphene, such as single, double and multiply vacancies. Recently, Vacancy defects in single sheet of graphene has been extensively studied by many researchers [98, 99, and 100]. Jing et al. [101] studied the effect of single and di-vacancy defects on the mechanical properties of single sheet of graphene. They predicted that di-vacancy defects are less detrimental to mechanical properties of graphene as compared to single vacancy defects. Jian et al. [102] performed molecular dynamics based simulations to study the effect of different vacancy configuration, size and concentration of vacancy defects on the mechanical properties of graphene. Gorjizadeh et al. [103] has proven that the thermal conductance of graphene deteriorates in defective graphene sheets. Banhart et al. [104] reviewed possible structural defects in graphene and their effects and potential applications. Parashar et al. [105] employed finite element based atomistic models to study the effect of non-bonded interactions on the fracture strength of graphene. They predicted

an overall improvement in the fracture toughness of graphene in presence of non-bonded interactions. Yuan et al. [106-107] employed molecular dynamics based simulation to study the structural stability of multiple sheets of graphene as well as sandwich structures of graphene with boron nitride.

In addition to deteriorating the mechanical properties of graphene, these defects has also been studied for modifying the failure behavior of graphene sheet [108]. Despite having exceptional mechanical properties, thermal and electrical conductivities, graphene sheet is limited with its applications due to brittle failure, exhibited by these sheets. In this article, authors has made an attempt to quantify the effect of non-bonded interactions on the failure mechanism as well as failure morphology of defected sheet of graphene accompanied by a pristine graphene sheet. An effort has been made to understand the transition in the failure mechanism of defective graphene sheets under the influence of non-bonded interactions in the bilayer configuration of graphene. During the simulations, non-bonded interactions as well as stiffness of pristine graphene was studied separately to quantify their impacts independently.

6.2 Details of molecular dynamics simulation based model

Molecular dynamics based simulations were performed to study the effect of non-bonded interactions on the mechanical behavior and failure morphology of defective graphene sheet. Success of any molecular dynamics-based simulations entirely depends on the interatomic potentials chosen for simulating the atomic interactions. Significant amount of advancement in conjunction with computational techniques has already been made by the researchers in developing potentials for capturing the realistic properties for the range of materials. In this study, AIREBO (adaptive intermolecular reactive bond order) potential was used to compute the interatomic forces between carbon atoms in graphene. Simulations were performed with single cutoff distance of 1.95Å as proposed in the work of [109]. AIREBO potential consists of summation of pair potential REBO (E_{ij}^{REBO}), non-bonded Lennard Jones potential (E_{ij}^{LJ}) and torsional component between carbon atoms (E_{ijk}^{tors}), also described with the help of mathematical expressions in Eqn (22) above recalling are mentioned below;

$$E^{AIREBO} = \frac{1}{2}\sum_i \sum_{i\neq} \left[E_{ij}^{REBO} + E_{ij}^{LJ} + \sum_{k\neq i,j} \sum_{l\neq i,j,k} E_{ijk}^{ltors} \right], \quad (23)$$

Here, i, j, k and l refers to individual atoms, E is the total potential energy of the system estimated with the help of AIREBO potential., In order to perform this study a graphene sheet consisting of 800 atoms was generated in the simulation box. The dimensions of single sheet of graphene was kept fixed at 46.599Å and 49.19Å (as shown in Fig.1) along the zig-zag and arm chair direction respectively. In plane periodic boundary conditions were imposed on the simulation box. The interlayer spacing between the sheets of graphene in bilayer graphene was kept at 3.45Å. During the simulations, NPT (isothermal- isobaric) ensemble in conjunction with an integration time step of 1fs was enforced. After achieving a minimum energy configuration of graphene, atoms at a temperature of 1K, tensile loading was applied at a strain rate of 0.005ps^{-1}. In order to avoid thermal effects on the failure mechanism of graphene, simulations were performed at such a low temperature of 1K. Stress strain response was estimated in this study with the help of virial stress component [110, 111], which can be calculated with the help of mathematical expression given in Eqn… (7), above are used again;

$$\sigma_{ij}^{\alpha} = 1/v(\frac{1}{2}m^{\alpha}v_i^{\alpha}v_j^{\alpha} + \sum_{\beta=1,n} r_{\alpha\beta}^{j}\ f_{\alpha\beta}^{i})\,; \tag{24}$$

Here, i and j denote indices in Cartesian coordinates system; α and β are the atomic indices; m^{α} and v^{α} are mass and velocity of atom α; $r_{\alpha\beta}$ is the distance between $\alpha\ and\ \beta$ atoms and V is the surrounding volume of atom α.

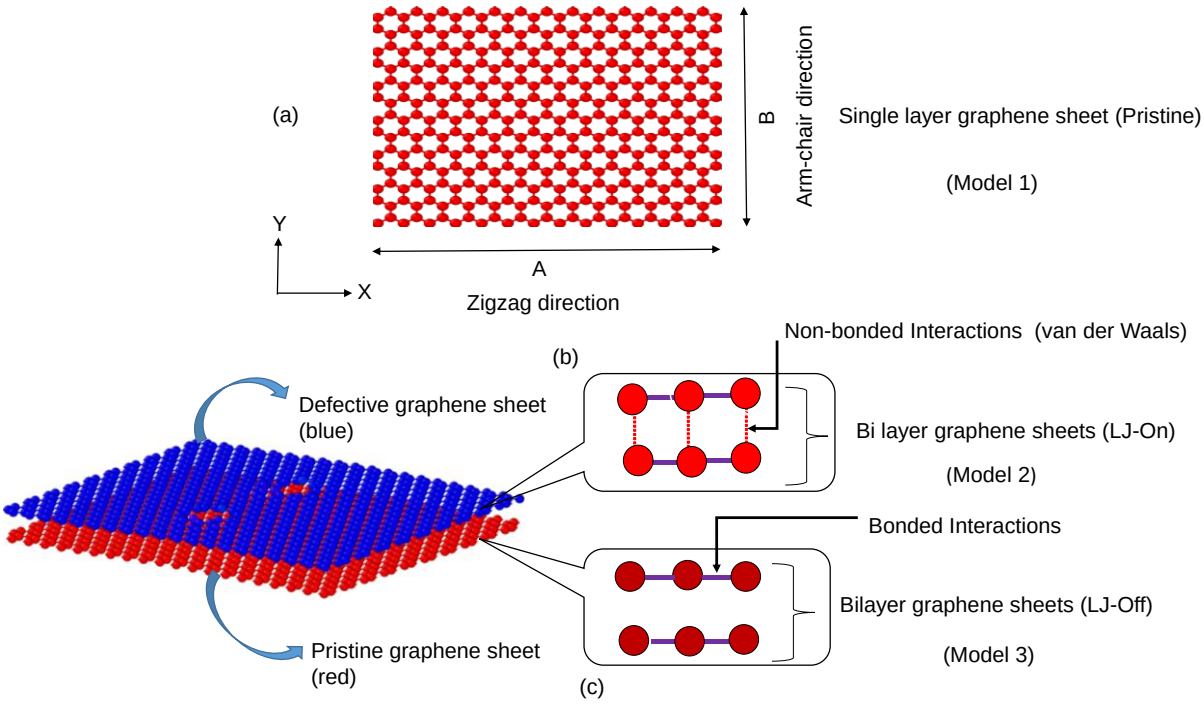

Figure 21. (a) Single sheet of graphene with respective direction also refereed as model #1 (b) schematic representation of non-bonded interactions between bi-layer configuration of graphene containing one defective and another pristine sheet, referred as model #2 (c) schematic representation of bi-layer configuration of graphene containing one defective and another pristine that without non-bonded interactions, referred as model #3.

Stacking sequence of multiple graphene sheets has been accounted in the article. Two different stacking sequences AA and AB (shown in Fig.21) has been considered in the simulations. It has already been established that graphene with AB stacking has more stable configuration as compared to AA [112]. In the simulations with non-bonded interactions between the bi-graphene sheets, the system energy minimized with AB stacking sequence. A uniform distribution of vacancy defects in the graphene sheet is considered for the simulation. The spacing between the defects was maintained in such a way that stresses developed around one vacancy defect will not get interacted with the stress field of neighbor vacancy defect.

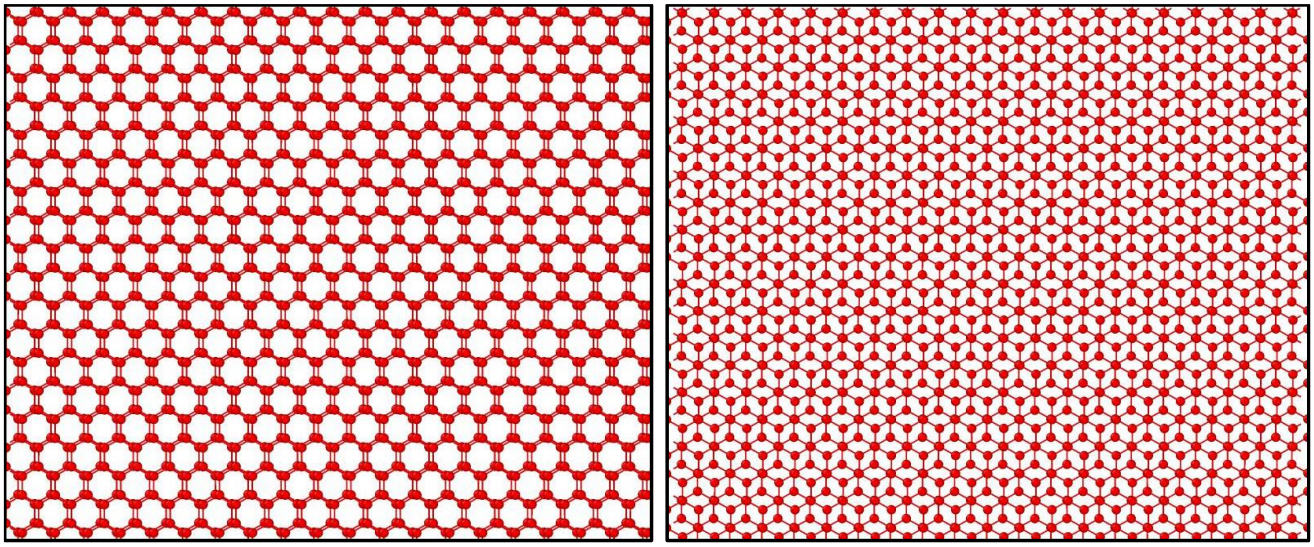

Figure 22. AA and AB stacked bi-layer graphene structure

Details of different types of atomistic models that were developed in molecular dynamics based environment are discussed below.

First model (Fig.20a): This represents single graphene sheet either pristine or defective (containing vacancy defects). Strength and failure morphology obtained from the simulation of single pristine sheet of graphene was further used as reference.

Second model (Fig.20b): Bi-layer sheets of graphene with an interlayer spacing was developed in molecular dynamics. Schematic representation of this model with two single sheets of graphene with van der Waals interactions between them is shown in Fig.20b. In this model, one graphene sheet is in pristine form, while it is accompanied by a defective graphene sheet (vacancy defects). In this model the interlayer spacing between the graphene sheets has been minimized for energy, which resulted in AB stacking sequence as shown in Fig.21. After minimization the interlayer spacing is maintained at 3.41Å. Particularly this model has been developed to study the effect of non-bonded interaction as well as stiffness of pristine graphene on the failure morphology or mechanism of defective graphene sheet. This model is now referred as BG (LJ-on) in rest of the paper.

Third model (Fig.20c): Once again, bilayer sheets of graphene were used to develop this model. In order to study the independent impact of stiffness of pristine graphene on the failure morphology or mechanism of defective graphene the non-boned interactions were kept switched off as shown in the schematic (Fig.20c). As non-bonded interactions between the layers of graphene is neglected, hence, the system energy minimized with AA stacking. This model is further referred as BG (LJ-off) in rest of the paper.

6.3 Results and discussion

Molecular dynamics based simulations were performed to capture the failure morphology of pristine graphene either as a single or in bi-layer sheet configuration. These simulations were performed with the help of three models discussed above to study the effects of non-bonded interactions on the mechanical behavior of pristine graphene. Stress and strain response estimated along the zig-zag and arm chair directions of pristine graphene are plotted in Fig.22. It can be observed from Fig.22 that the mechanical properties of pristine graphene is not affected by the non-bonded interactions.

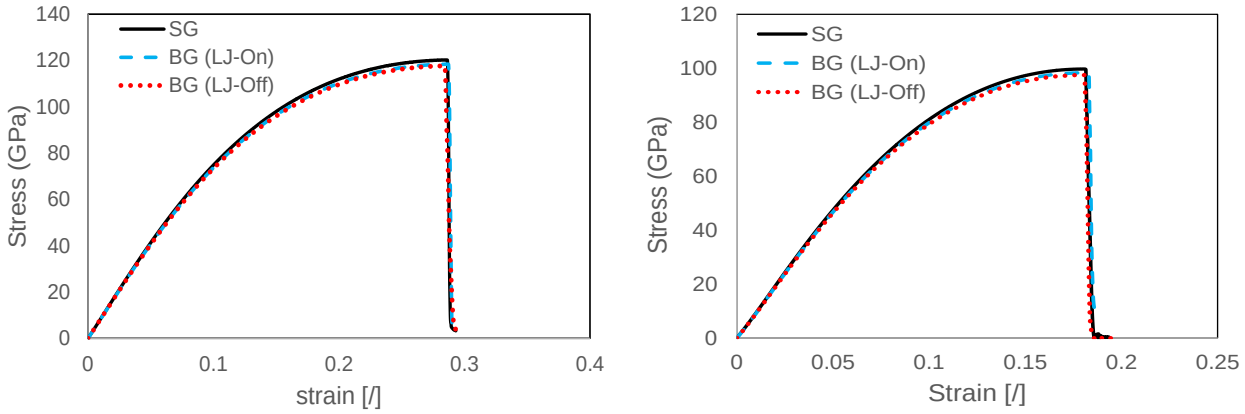

Figure 23. Stress-strain curves of pristine graphene under (a) zigzag and (b) armchair direction; where SG (single graphene sheet), BG (LJ-On) (bilayer graphene sheet with non-bonded interactions) and BG (LJ-Off) (bilayer graphene without non-bonded interactions).

In order to get a better insight on the failure mechanism of the pristine form of graphene under the influence of tensile loading, snapshots of the simulation box were taken at the time of initiation of the failure as provide in Fig.23.

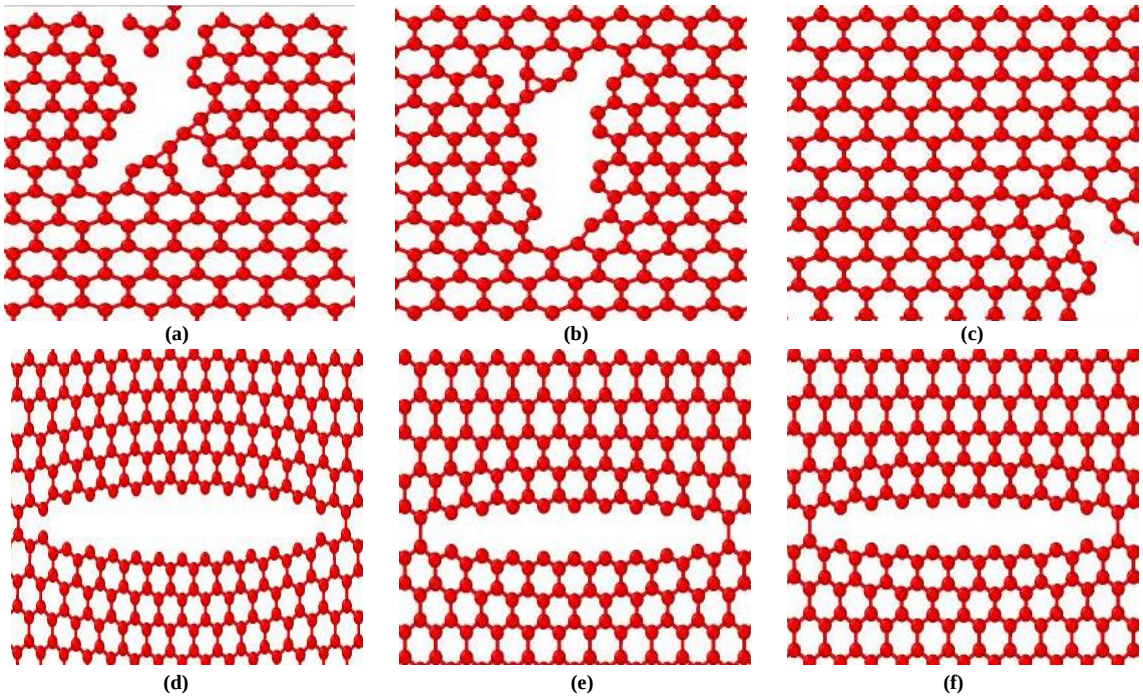

Figure 24. Failure morphology of pristine single and bilayer sheets (a &d) along zig-zag and arm chair directions with model #1 respectively (b & e) along zig-zag and arm chair directions with model #2 (c & f) along zig-zag and arm chair directions with model #3.

It can be seen that the failure morphology of graphene sheet in Fig.23 is almost independent to the non-bonded interactions. A brittle nature of failure can be observed in zig-zag as well as arm chair directions of graphene sheets under the influence of tensile loading.

6.4 Effect of defect concentration on the failure mechanism of graphene

Simulations were performed with varying concentration of single vacancy defects in single and bilayer sheets of graphene. Mechanical properties and failure morphology of graphene was studied with the help of three models defined in the previous section (model #1, model #2 and model#3). Separate simulations were performed with zig-zag and arm chair configurations of the graphene sheets. Initially, simulations were performed with the single sheet of graphene with varying concentration of single vacancy defects in graphene. After performing the simulations with single sheet of defective graphene, simulations were performed with bilayer sheets of graphene with the help of model #2 (non-bonded interactions were considered between the defective and pristine graphene) and model #3 (non-bonded interactions were not considered between the defective and pristine graphene). In order to capture the effect of non-bonded interactions as well as the stiffness of pristine sheet in bilayer configuration of graphene on the defective graphene, failure strength as well as strain was recorded only for the defective sheet in all the simulations. Failure strength and strain predicted for the defective graphene sheet (either single or accompanied by pristine graphene in bilayer) under the influence of tensile load in zig zag direction is plotted in Fig.24.

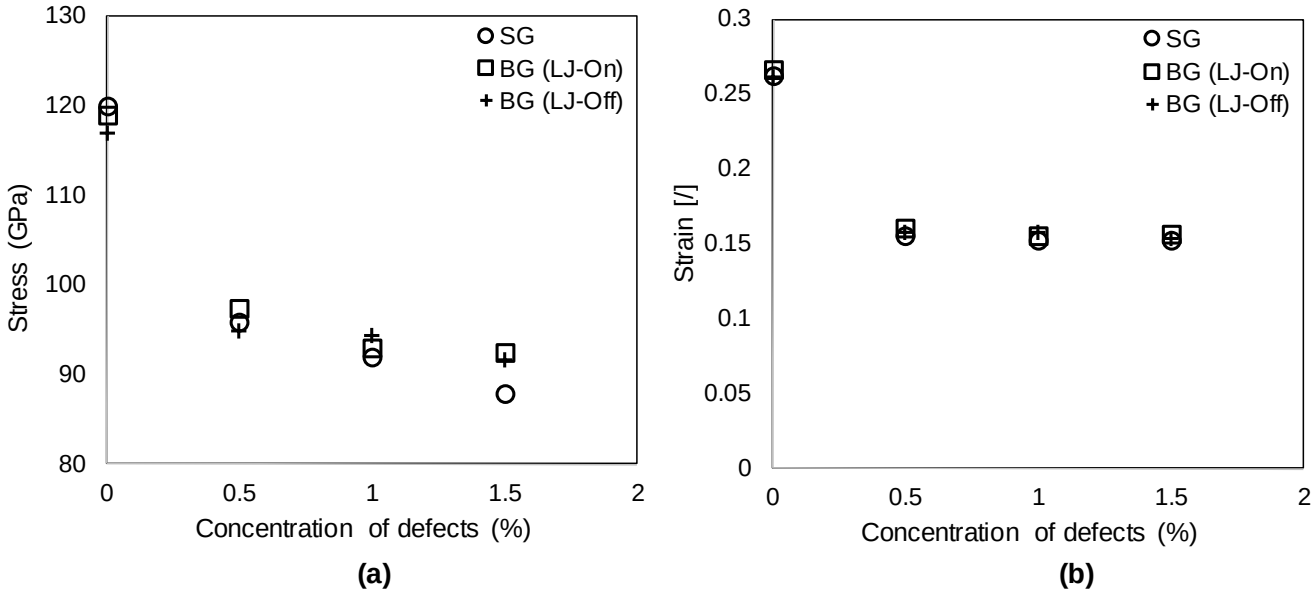

Figure 25. (a) Fracture stress (b) fracture strain of graphene sheets while subjected to tensile loading align with the zig-zag direction of graphene.

It can be observed from Fig.24a that up to 1.0 % concentration of vacancy defects, no significant difference in terms of fracture strength has been observed in defective sheet of graphene, while comparing single defective graphene sheet with BG (LJ-on) and BG (LJ-off) models of bilayer configuration of graphene. On the other hand, at 1.5% concentration of single vacancy defects, defective graphene in BG (LJ-on) and BG (LJ-off) has shown slight improvement in strength as compared to isolated defective sheet of graphene. Overall, less than 5% improvement in the fracture strength of defective graphene was observed, while modelling the defective sheet next to a pristine sheet connected with non-bonded interaction, BG (LJ-on), whereas almost similar improvement was also observed with bilayer graphene sheets without non-bonded interactions, BG (LJ-off), at the same % concentration of vacancy defects. It helps in identifying the fact that the stiffness of pristine graphene in bilayer configuration of graphene is having more contribution as compared to non-bonded interactions in improving the strength of defective graphene. No significant variation in the fracture strain is observed for zig-zag configuration of graphene with model #2 and model #3. In order to get a better insight on the influence of the non-bonded interactions, as well as stiffness of pristine graphene on the failure morphology of defective sheets, snapshots taken at the initiation of failure along the zig-zag direction is provided in Fig.25.

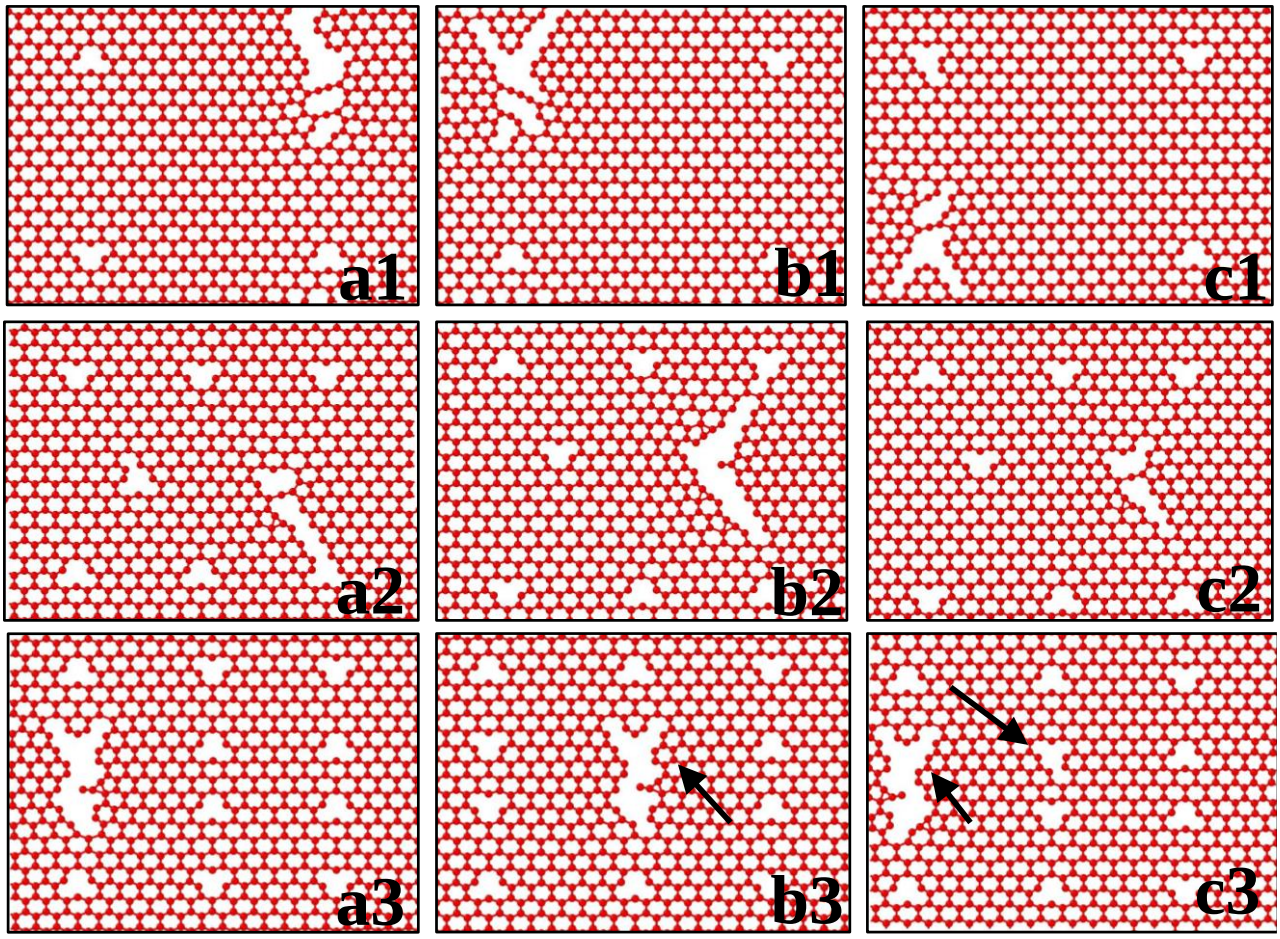

Figure 26. Failure morphology of zig-zag configuration of defective graphene with varying concentration of single vacancy defects, (a1 to a3) failure morphology of defective graphene with model #1 (a1)-0.5%, (a2) 1.0% and (a3) 1.5%, (b1 to b3) failure morphology of defective graphene with model #2 (b1)-0.5%, (b2) 1.0% and (b3) 1.5%, (c1 to c3) failure morphology of defective graphene with model #1 (c1) 0.5%, (c2) 1.0% and (c3) 1.5%.

It can be inferred from Fig.24 that non-bonded interactions as well as stiffness of pristine graphene are important for the failure morphology of defective graphene sheet. Snapshots of the simulation box provided in Fig.25 (c3) for defective graphene sheet in BG (LJ-on) with 1.5% vacancy defects indicates that the failure initiates at two different region, subsequently and helps in achieving a higher failure strength. This initiation of failure at two different location helps in distributing the energy among these points, which can be attributed for the slightly higher failure strength for defective graphene sheets in bilayer configuration connected with non-bonded interactions.

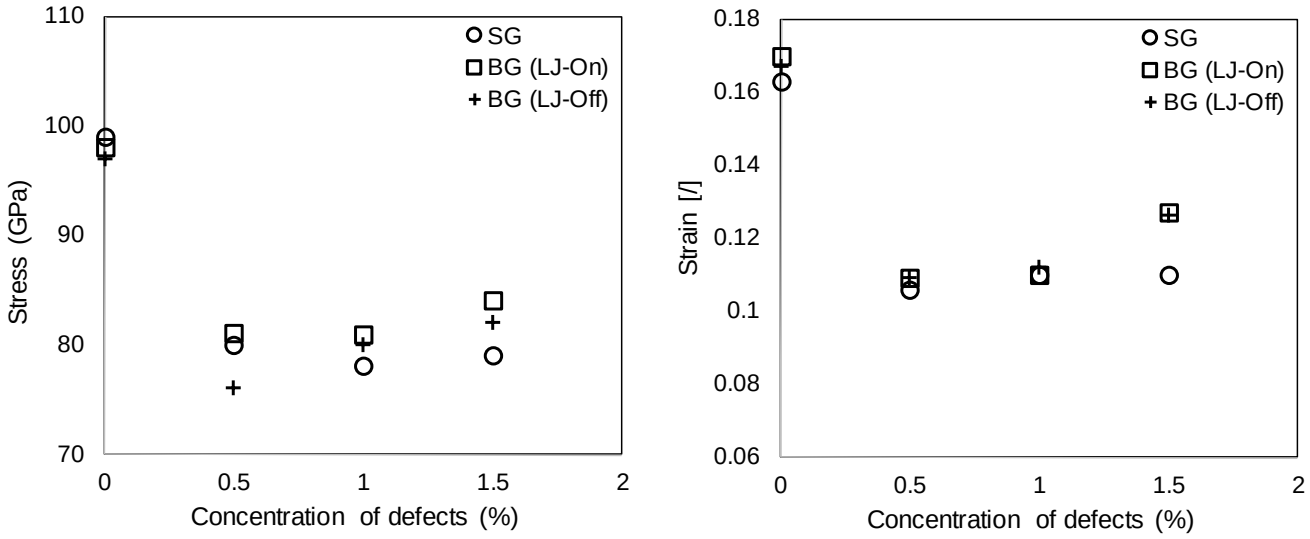

Figure 27. (a) Fracture stress (b) fracture strain of graphene sheets while subjected to tensile loading align with the arm chair direction of graphene.

Similar to zig-zag direction, improvement in the failure strength of defective graphene was also observed along the arm chair direction with higher percentage of single vacancy defects as shown in Fig.26. Maximum improvement of 6.5% is observed in fracture strength of defective graphene when it was connected with pristine graphene with non-bonded interactions that is represented by BG (LJ-on). Similar to strength, improvement in fracture strain was also observed in arm chair direction at 1.5% concentration of single vacancy defects. Significant improvement of 15% is observed in fracture strain at 1.5% concentration of single vacancy defects for defective graphene in bilayer configuration as shown in Fig.26b.

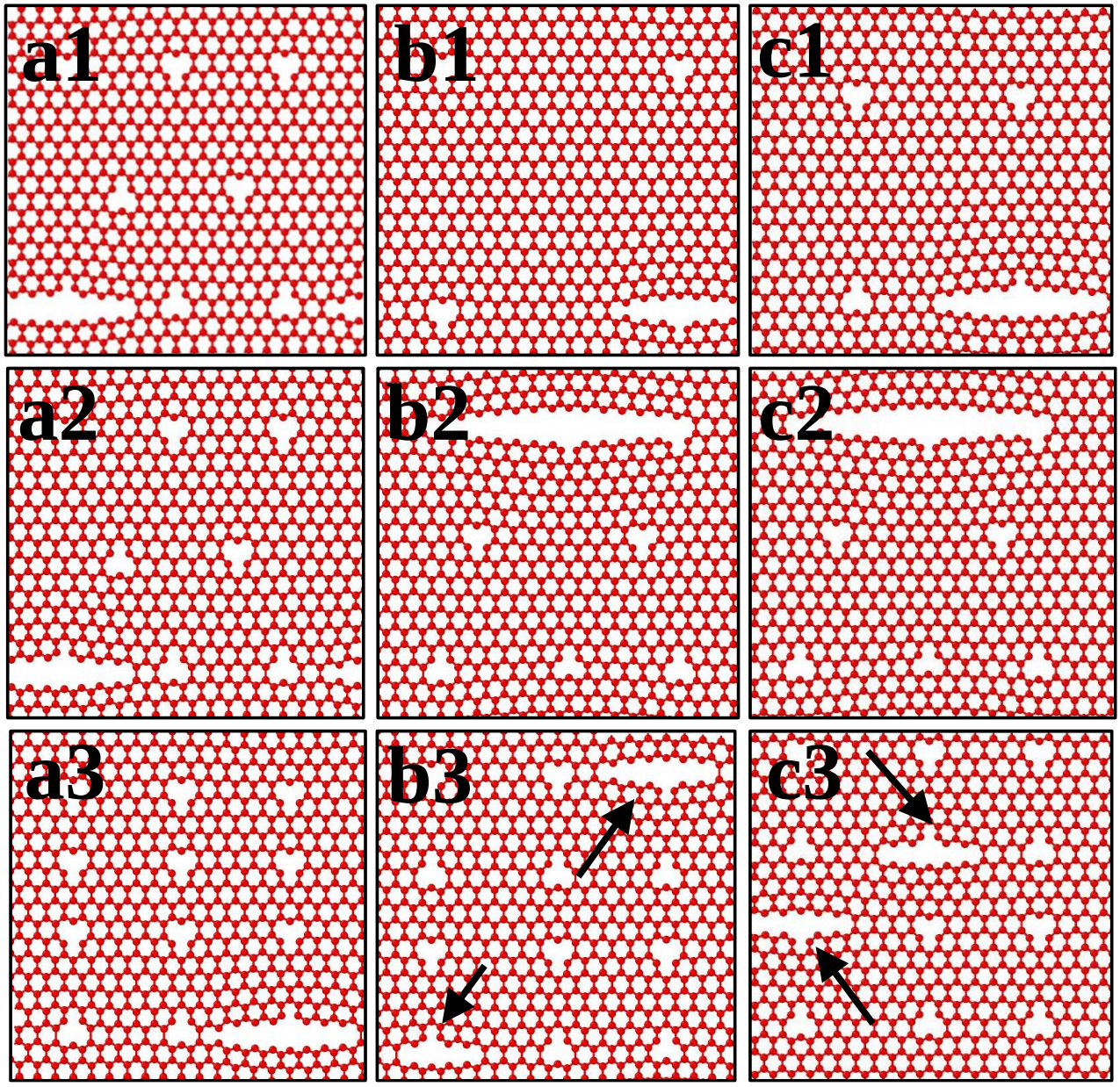

Figure 28. Failure morphology of arm chair configuration of defective graphene with varying concentration of single vacancy defects, (a1 to a3) failure morphology of defective graphene with model #1 (a1)-0.5%, (a2) 1.0% and (a3) 1.5%, (b1 to b3) failure morphology of defective graphene with model #2 (b1)-0.5%, (b2) 1.0% and (b3) 1.5%, (c1 to c3) failure morphology of defective graphene with model #1 (c1)-0.5%, (c2) 1.0% and (c3) 1.5%.

In order to investigate the physics behind the improvement in the fracture strength and strain of defective graphene in bilayer configuration of graphene, snapshots at the time of initiation of failure is considered in Fig.27. It can be observed in Fig.27 (b3 and c3) that at the higher concentration of single vacancy defects (1.5%) failure triggers from the vacancies at two separate

locations. Distribution of loading with the help of non-bonded interactions as well as pristine graphene sheet accompanied the defective graphene can be attributed to the higher strength of defective graphene in bi-layer configuration of graphene. Molecular dynamics based simulation helps in concluding that at higher percentage of single vacancy defects, bilayer sheets of graphene shows higher strength and strain values for the failure of defective graphene sheet. Improvement in the strength of defective sheet was observed in the presence of another sheet of pristine graphene connected together with non-bonded interactions, but no transition from brittle behavior was observed in the failure morphology.

6.5 Effect of single, double and multiple vacancy defects

In addition to the percentage concentration of vacancy defects, simulations were also performed with different type or geometries of vacancy defects starting from single, double and multiple vacancy defects. In this subsection, concentration of vacancy defects was kept constant at 1.5%, but the geometry of vacancy defects were varied from single to double and multiple vacancies (6 atoms removed from a single place) as shown in Fig.9. In this subsection simulations were performed only with model #1 (isolated defective graphene) and model #2 (defective graphene in bilayer configuration connected with pristine graphene via non-bonded interactions) that is BG (LJ-on).

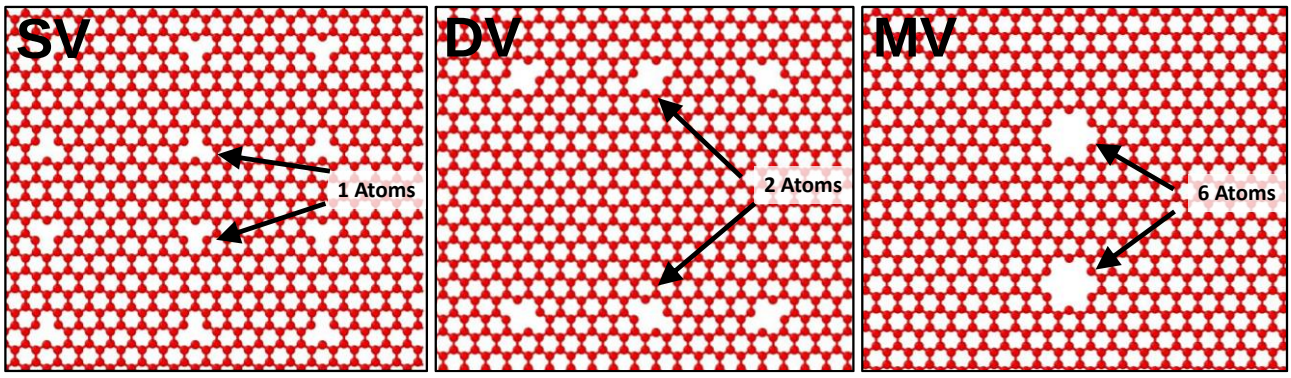

Figure 29 .Snapshots taken from the simulation box with different geometry of vacancy defects at the same concentration. Here in the snapshots, SV, DV and MV refers to single vacancy double vacancy and multiple vacancy defects.

Failure strength and strain obtained from simulations performed with single, double and multiple vacancy defects lying in single sheet of graphene as well as in BG (LJ-on) are provided in Fig.29, while the direction of tensile loading was align with the zig-zag direction.

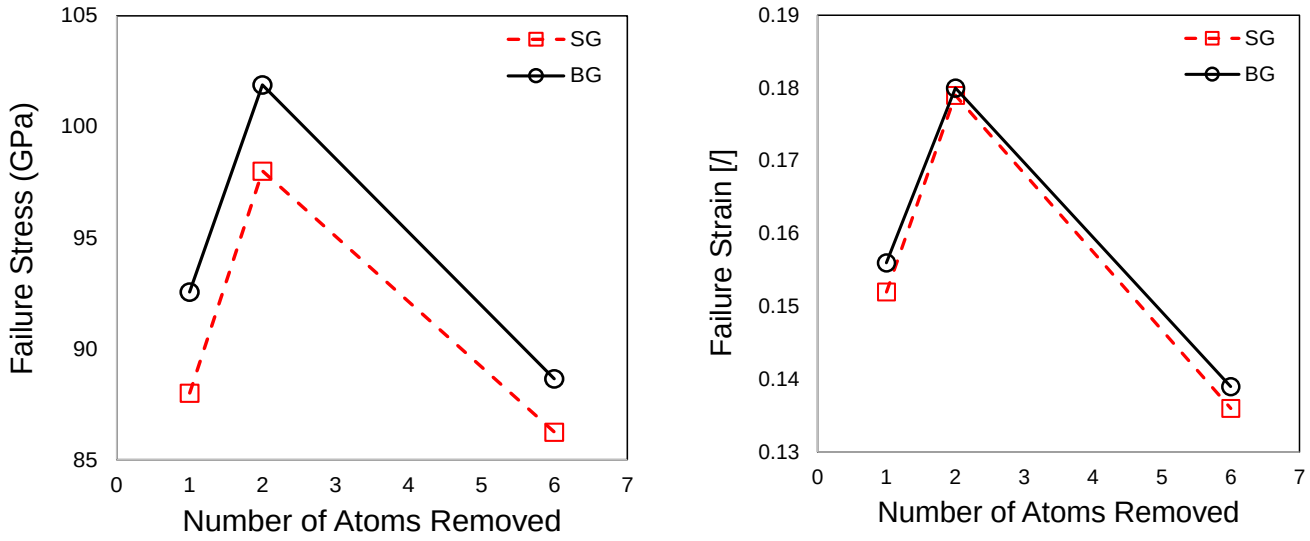

Figure 30. Failure stress and strain for single, double and multiple vacancy defects modeled with isolated single sheet of graphene (model #1) as well as with bilayer sheets of graphene (model#2) along the zig-zag direction. SG and BG refers as single sheet and bilayer sheet of graphene respectively.

It can be predicted from Fig.29 that failure stress increases for a defective sheet of graphene in a bilayer configuration of graphene that is BG (LJ-on). Same concentration of defects has generated different failure stress and strain with single, double and multiple vacancy defects. Double vacancy defects can be inferred more stable as compared to single and multiple vacancy defects. Bilayer configuration of graphene has produce higher failure strength as compared to single defective graphene sheet. In order to study the physics behind the increase in failure strength of defective sheet in bilayer configuration of graphene, snapshots taken from the simulation box at different time steps are provide in Fig. 30 and Fig.31 with di-vacancy and multi-vacancy defects respectively.

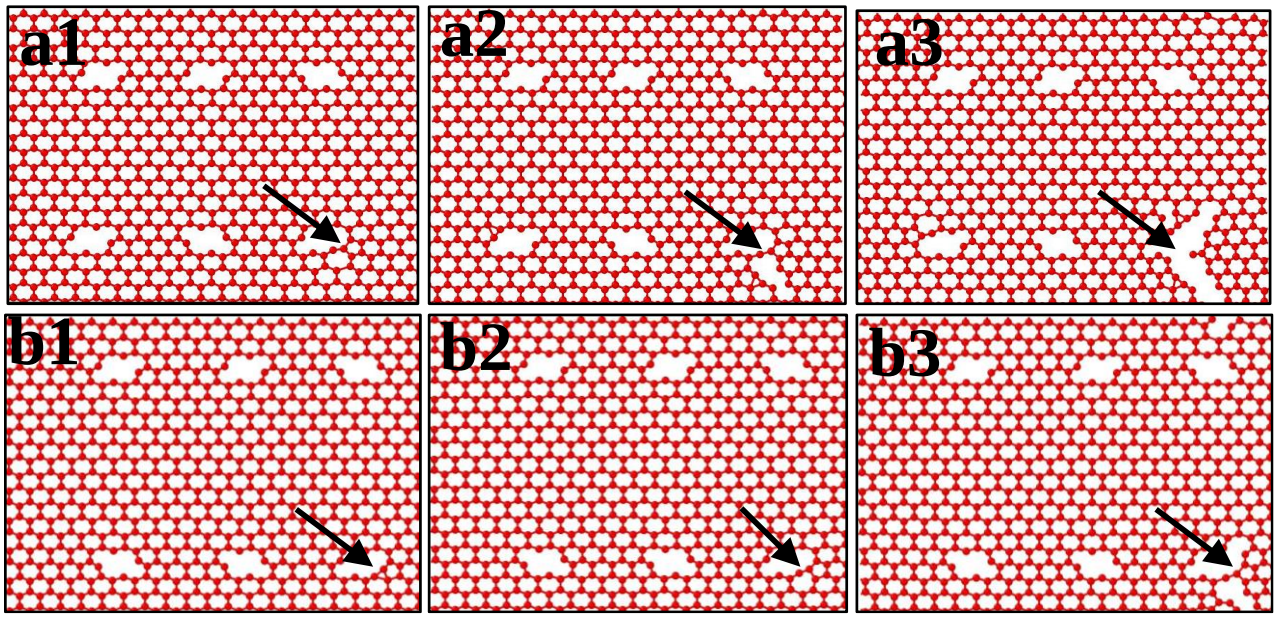

Figure 31. Failure morphology with single sheet as well as bilayer sheets of graphene along the zigzag direction containing double vacancies in defective sheet. (a1-a3) failure morphology of di-vacancy defects in at increasing time step in an isolated sheet of graphene (b1-b3) failure morphology of di-vacancy defects in at increasing time step in a bilayer graphene.

Failure morphology of single isolated defective graphene sheet (model #1) as well as defective sheet in bilayer configuration of graphene containing di-vacancy defects can be further studied with the help of progress in failure provided in Fig.30. Failure morphology of single defective sheet as well as defective sheet in bilayer configuration are shown in Fig.30 (a1 to a3) and Fig.30 (b1 to b3) respectively. In both the cases with isolated sheet of graphene as well as with -bilayer configuration, it can be inferred that failure morphology under the influence of tensile loading along the zig-zag direction is almost same. Initially, bond breaking takes place at the edge of di-vacancy defect, which further triggers the formation of 5-7 stable configuration at the same edge and helps in sustaining more load before the final failure.

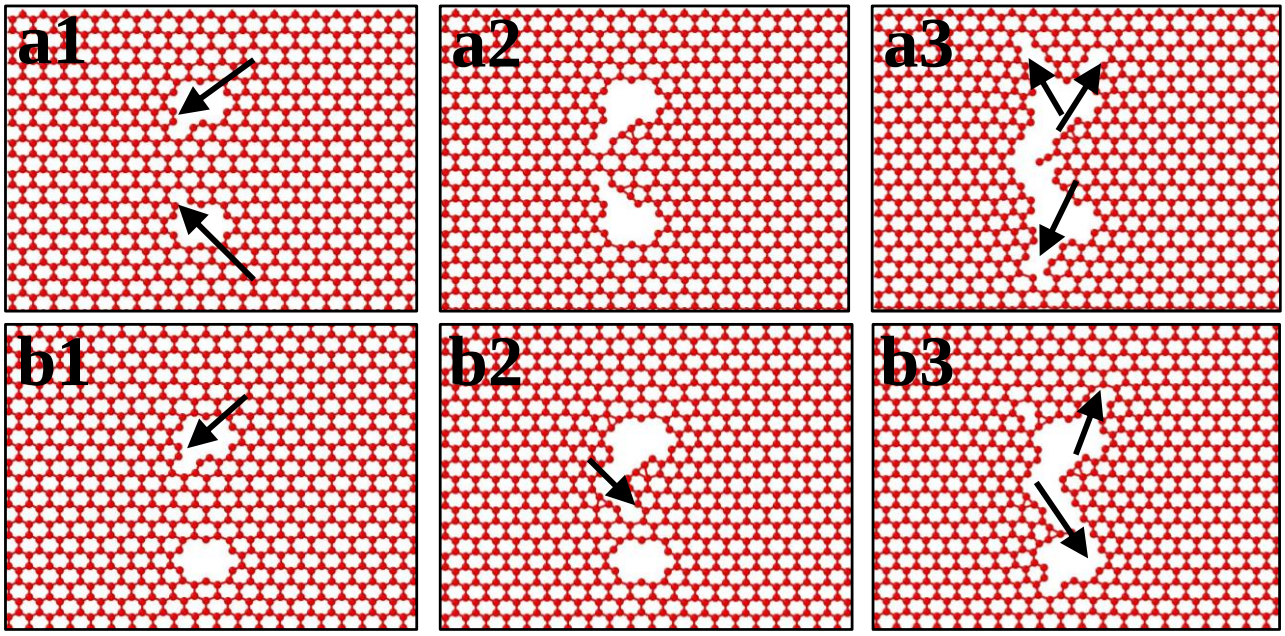

Figure 32. Failure morphology with single sheet as well as bilayer sheets of graphene along the zigzag direction containing multiple vacancies in defective sheet. (a1-a3) failure morphology of multiple vacancy defects in at increasing time step in an isolated sheet of graphene (b1-b3) failure morphology of multiple vacancy defects in at increasing time step in a bilayer graphene.

Failure morphology of graphene containing multi-vacancy defects either in isolated or bilayer configuration of graphene (BG (LJ-on)) is shown in Fig.31. It can be inferred from the snapshots in Fig.31 that multiple vacancy defects eventually weaken the strength of graphene, hence have minimum strength as compared to single and di-vacancy defects.

No noticeable change in failure morphology as well as strength was predicted for isolated sheet of graphene as well as defective sheet in bilayer configuration of graphene containing multi-vacancy defects. In addition to these snapshots of failure morphology, average value of maximum force obtained over 50 integration time steps are shown in Fig.32. In Fig.32, force acting in line with the direction of loading is plotted. Zig zag and arm chair direction are considered to be align with ‘X’ and ‘Y’ coordinates of the model.

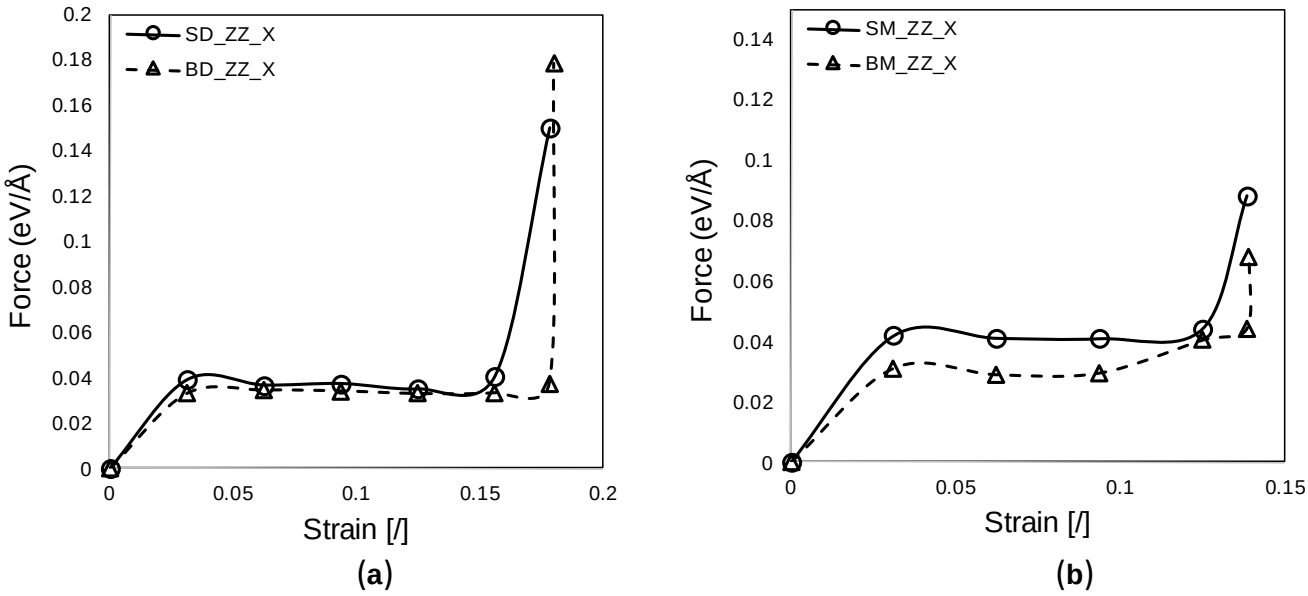

Figure 33. Average maximum atomic force along zig zag direction of graphene with (a) di-vacancy defects, SD and BD refers to single and bilayer configuration of graphene (b) multi-vacancy defects, SM and BM refers to single and bilayer configuration of graphene.

No significant variation in maximum force component is observed from Fig. 32 with respect to single and bilayer configuration of graphene containing bi-vacancy as well as multi-vacancy defects. This trend in Fig.32 is further validated the failure morphology reported in Fig.30 and Fig.31, which also indicates towards the same failure morphology with single and bilayer configuration graphene.

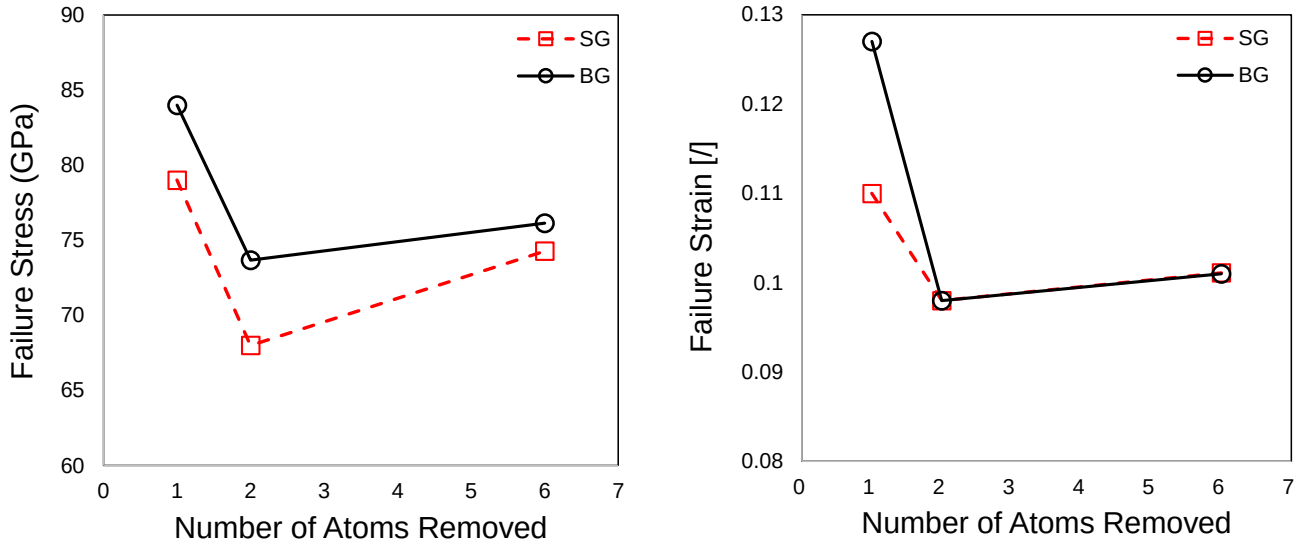

Figure 34. Failure stress and strain for single, double and multiple vacancy defects modeled with isolated single sheet of graphene as well as with bilayer sheets of graphene (model#2) along the arm-chair direction. SG and BG refers as single sheet of graphene and bilayer sheet of graphene with non-bonded interactions respectively.

Similar to zig-zag direction of loading, simulations were also performed with arm chair direction of graphene. It can be seen in Fig.33 that as compared to single and multiple vacancy defects, graphene containing di-vacancy sheets have shown lower strength when the load is applied along the arm chair direction. Once again the defective sheet in bilayer configuration of graphene has shown a better strength as compared to an isolated defective sheet of graphene. Despite the fact that di-vacancy defects have lower strength as compared to single vacancy along the arm chair direction, the bilayer configuration of graphene has shown a significant improvement over the strength of defective graphene. An overall increase of 9% is predicted for the failure strength of defective graphene in bi-layer configuration as compared to the strength of isolated defective graphene sheet. In addition to failure stress and strain, failure morphology was also studied with the help of Fig. 34 and Fig. 35.

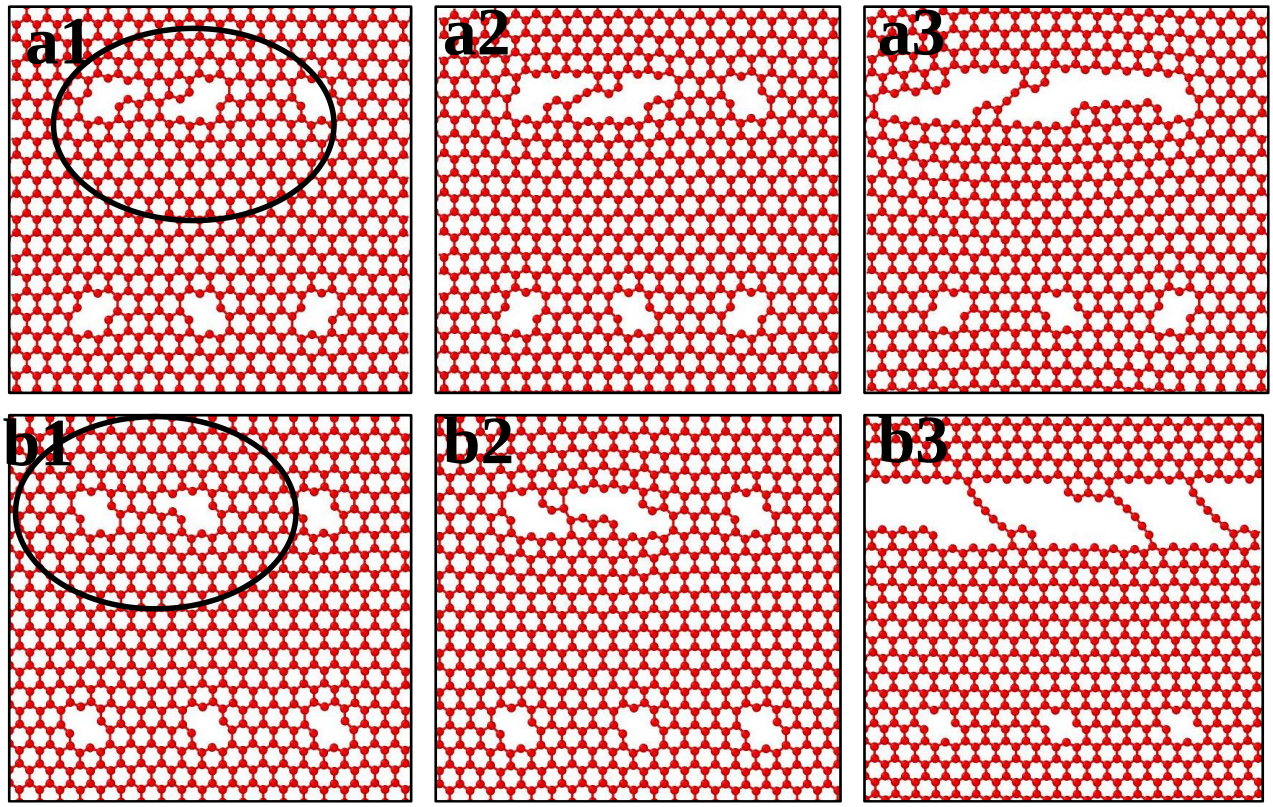

Figure 35 .Failure morphology with single sheet as well as bilayer sheets of graphene along the arm-chair direction containing double vacancies in defective sheet. (a1-a3) failure morphology of

di-vacancy defects in at increasing time step in an isolated sheet of graphene (b1-b3) failure morphology of di-vacancy defects in at increasing time step in a bilayer graphene

Failure morphology of single as well as defective graphene in bilayer configuration along the arm chair direction at the time of initiation is shown in Fig.34 and Fig.35 for di-vacancy and multi vacancy defects respectively. It can be inferred from Fig.34 (a1 to a3) and Fig. 34 (b1 to b3) that the bond breaking starts simultaneously for to di-vacancy defects both in isolated defective as well as bilayer sheet of graphene. Transition in the failure morphology can be seen in defective graphene sheets of graphene in bilayer configuration of graphene as compared to isolated sheet of graphene. Brittle nature of failure with the nature of bond breaking can be observed in Fig.34 (a3), while the shift in the failure morphology from brittle to mild ductile is predicted in bi-layer configuration of defective graphene that is BG (LJ-on). Defective sheet of graphene in BG (LJ-on) has shown chain formation at the failure sites which helps in modifying the failure morphology as well as the overall strength of defective graphene as well. More chains were formed in Fig.33 (b3) as compared to Fig.33 (a3), which eventually modifies the failure mode to ductile one from the brittle.

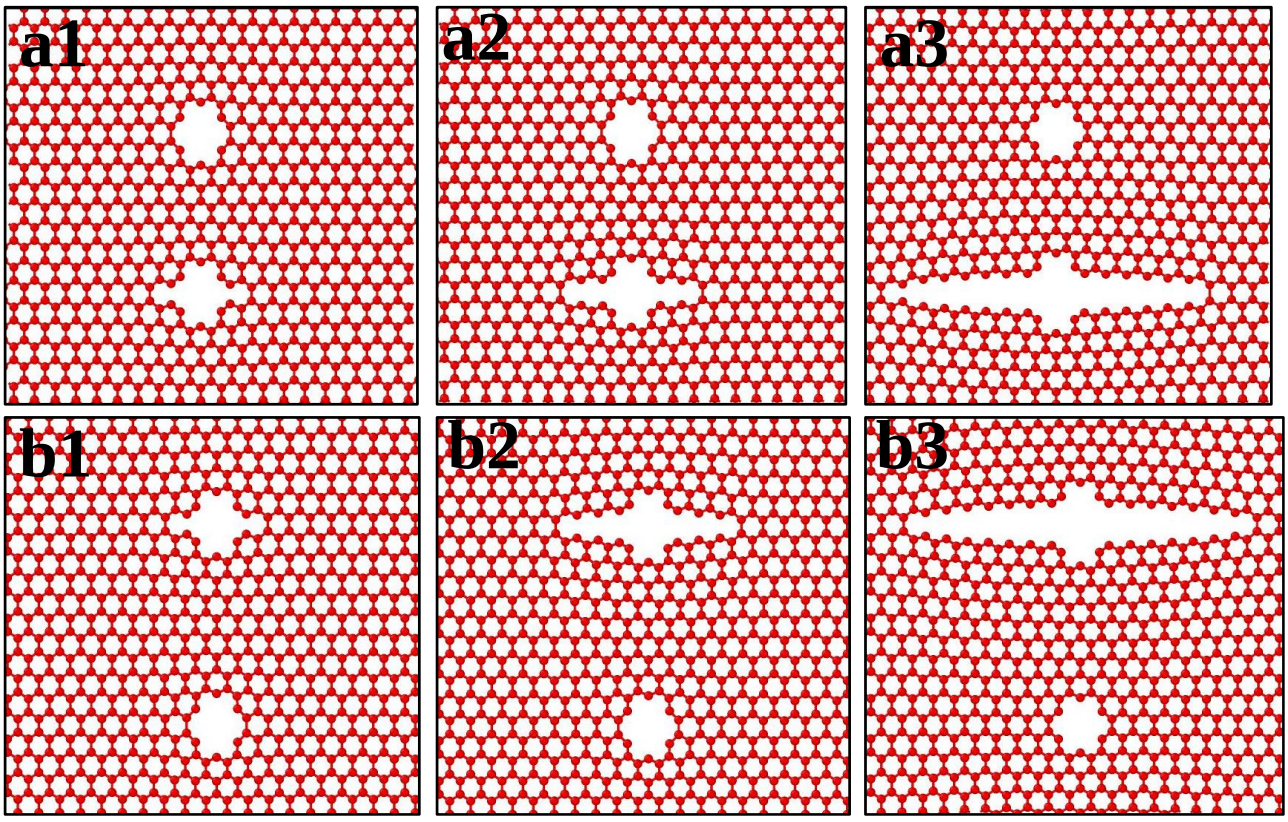

Figure 36. Failure morphology with single sheet as well as bilayer sheets of graphene along the arm-chair direction containing multiple vacancies in defective sheet. (a1-a3) failure morphology of multiple vacancy defects in at increasing time step in an isolated sheet of graphene (b1-b3) failure morphology of multiple vacancy defects in at increasing time step in a bilayer graphene

Similar to zig-zag direction of loading, arm chair configuration of graphene with multi-vacancy defects have shown no variation in failure morphology with non-bonded interactions as shown in Fig.35.

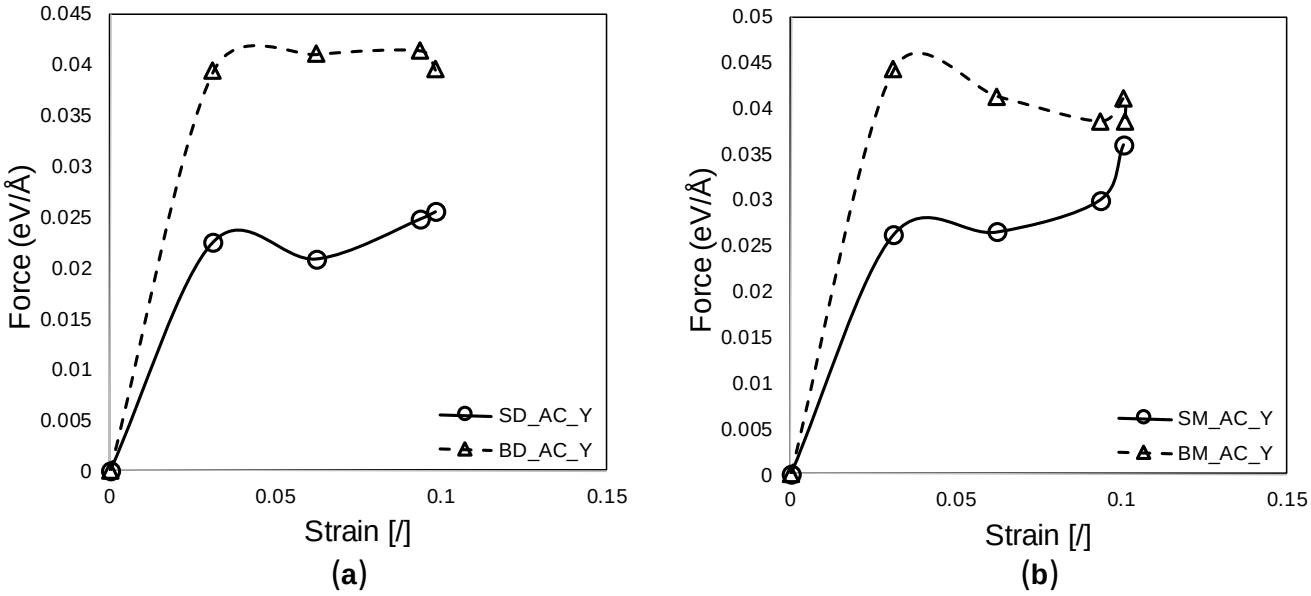

Figure 37.Average maximum atomic force along arm-chair direction of graphene with (a) di-vacancy defects, SD and BD refers to single and bilayer configuration of graphene (b) multi-vacancy defects, SM and BM refers to single and bilayer configuration of graphene.

Average atomic force along the arm chair direction of loading is plotted in Fig. 36 for both di-vacancy and multi-vacancy defects. Higher degree of local force vector can be observed for bilayer configuration of graphene as compared to single defective sheet of graphene. This further emphasis a higher failure strength for defective sheet of graphene in bilayer configuration.

CHAPTER 7

SUMMARY AND CONCLUSIONS

7.1 Summary of the current work and main results

Systematic Molecular Dynamics simulation (MDs) would be carried out to study the mechanical properties of vacancy defective graphene from different position. This work based on the effect of defects; on the mechanical properties and crack behavior of graphene has been carried out to study structural-property relation, following value added points are derived from this study,

1. It is found that vacancy defects (VDS) can weaken the strength of graphene, where impact of VDs is more significant due to higher number of dangling bonds.
2. It can be concluded that σf of graphene depends on number of VDs, distance between the vacancy defects and temperature.
3. Effect of vacancy defects on the strength of graphene sheets have been investigated so that it was found that finiteness of a defective graphene sheet has a significant influence on the MD simulations that, MD simulation outcomes specified that vacancy defect can reduce the strength of graphene sheet.
4. A single vacancy defect (one missing of atom) could diminish the strength of graphene sheet by around 20%. Therefore, it is very important to reduce the defects in graphene sheets during production stage, especially for sheets which will be used for structural applications.
5. Molecular dynamics based simulations were performed to predict the effect of non-bonded interactions on the mechanical behavior and failure morphology of defective graphene sheet so that simulation were performed with an isolated defective sheet of graphene or defective sheet of graphene accompanied by a pristine sheet of graphene.

6. Atomistic modeling with single as well as bilayer configuration of graphene was performed with different defect concentrations as well as geometries of vacancy defects such as single, double and multiple vacancy defects.
7. Di-vacancy defects have predicted higher strength in zig-zag configuration, whereas lower strength in arm chair configuration while compared with the single vacancy defects.
8. Shifting the failure morphology of graphene along the arm chair direction was observed in bi-layer configuration of defective graphene containing di-vacancy defects.
9. It can be concluded that non-bonded interaction helps in achieving a uniform distribution of load around the defects which triggers the failure simultaneously from different regions and initiating of failure simultaneously from two different points help in achieving a higher strength.

7.2 Recommendations for future work

1. Therefore studying the future aspect of graphene defects, such as point vacancy, double vacancy and multi-vacancies will give an overall picture of the effects in vacancy defects on mechanical properties. After studying the double layer and triple layer defects we will compare with point vacancy, di-vacancy (DV) and multi-vacancy (MV) to give overall picture of the effects in VDs on mechanical properties. The better stability of the di-vacancy in its different configurations formation is of a particular importance.
2. Scaled stress explanation is incapable to arrest the local stress distribution around a crack of (vacancy defect) a graphene sheet. In reality, virial stress is also not a noble stress measure to calculate local atomic stresses. Analysis of stress concentration around the crack or defect tip of a graphene sheet can give a better insight of the effect of defects.
3. This thesis is primarily focused on the effect of defects. However, it has been found that vacancy defects have a profound impact on the strength and stiffness which create unstable on a material. Therefore, a study of the effect of vacancy-containing defects such as single vacancy, di- vacancy and multi-vacancy will give an overall picture of the effects of vacancy defect on mechanical properties of graphene.
4. Minding, the presence of defects significantly reduces the tensile strength. Overall, novel properties seem to decrease as the number of defects increases, this may be happen due to bond-bond interactions.

REFERENCES

1. Lovat, G., G. W. Hanson, R. Araneo, and P. Burghignoli. "Comparison of spatially dispersive models for dyadic intraband conductivity of graphene." In*Antennas and Propagation (EuCAP), 2013 7th European Conference on*, pp. 500-504. IEEE, 2013.
2. Sakhaee-Pour, A., Ahmadian, M. T., &Vafai, A. (2008). Applications of single-layered graphene sheets as mass sensors and atomistic dust detectors. Solid State Communications,
3. Sakhaee-Pour, A., Ahmadian, M. T., &Vafai, A. (2008). Applications of single-layered graphene sheets as mass sensors and atomistic dust detectors. Solid State Communications,
4. Liu, Bo, C. D. Reddy, Jinwu Jiang, Julia A. Baimova, Sergey V. Dmitriev, Ayrat A. Nazarov, and Kun Zhou. "Morphology and in-plane thermal conductivity of hybrid graphene sheets." *Applied Physics Letters* 101, no. 21 (2012): 211909.
5. Gillen, Roland, Marcel Mohr, Christian Thomsen, and JaninaMaultzsch. "Vibrational properties of graphene nanoribbons by first-principles calculations. *"Physical Review B* 80, no. 15 (2009): 155418.
6. Mohr, M., J. Maultzsch, E. Dobardžić, S. Reich, I. Milošević, M. Damnjanović, A. Bosak, M. Krisch, and C. Thomsen. "Phonon dispersion of graphite by inelastic x-ray scattering." *Physical Review B* 76, no. 3 (2007): 035439.
7. S.V. Dmitrriev, J.A. Baimoya, A.V. Savin, Y.S. Kivshar. Comput. Mater. Sci. 53 (2012) 194- 203.
8. Los, J. H., Mikhail I. Katsnelson, O. V. Yazyev, K. V. Zakharchenko, and Annalisa Fasolino. "Scaling properties of flexible membranes from atomistic simulations: application to graphene." *Physical Review B* 80, no. 12 (2009): 121405.
9. Gulino, Antonino. "Structural and electronic characterization of self-assembled molecular nanoarchitectures by X-ray photoelectron spectroscopy." *Analytical and bioanalytical chemistry* 405, no. 5 (2013): 1479-1495.
10. Kudernac, Tibor, NoppornRuangsupapichat, Manfred Parschau, Beatriz Maciá, Nathalie Katsonis, Syuzanna R. Harutyunyan, Karl-Heinz Ernst, and Ben L. Feringa. "Electrically driven directional motion of a four-wheeled molecule on a metal surface." *Nature* 479, no. 7372 (2011): 208-211.

11. Novoselov, K. S., D. Jiang, F. Schedin, T. J. Booth, V. V. Khotkevich, S. V. Morozov, and A. K. Geim. "Two-dimensional atomic crystals." Proceedings of the National Academy of Sciences of the United States of America 102, no. 30 (2005): 10451-10453.
12. Newson, Ryan W., Jesse Dean, Ben Schmidt, and Henry M. van Driel. "Ultrafast carrier kinetics in exfoliated graphene and thin graphite films." *Optics express* 17, no. 4 (2009): 2326-2333.
13. Parashar, Avinash, and Pierre Mertiny. "Multiscale model to investigate the effect of graphene on the fracture characteristics of graphene/polymer nanocomposites." Nanoscale research letters 7, no. 1 (2012): 1-8.
14. H.M.Tu, S.H, Huh, S.H.Choi, andH.L.Lee structures of thermally and chemically reduced graphenes, Mater-lett, 64 (2010).
15. An, F. P., J. Z. Bai, A. B. Balantekin, H. R. Band, D. Beavis, W. Beriguete, M. Bishai et al. "Observation of electron-antineutrino disappearance at DayaBay. *"Physical Review Letters* 108, no. 17 (2012): 171803.
16. Lv, Wei, Min Guo, Ming-Hui Liang, Feng-Min Jin, Lan Cui, LinjieZhi, and Quan-Hong Yang. "Graphene-DNA hybrids: self-assembly and electrochemical detection performance." *J. Mater. Chem.* 20, no. 32 (2010): 6668-6673.
17. Hai-Yang, Song, and Zha Xin-Wei. "Mechanical properties of Ni-coated single graphene sheet and their embedded aluminum matrix composites. *"*Communications in Theoretical Physics 54, no. 1 (2010): 143.
18. A.W. Cummings, D.L. Duong, V.L. Nguyen, D.V. Tuan, J. Kotakoski, J.E.B. Varga, Charge Transport in Polycrystalline Graphene: Challenges and Opportunities, *Adv. Mater.*, 26, 5079-5094
19. C. Lee, X. Wei, J. W. Kysar, and J. Hone, Measurement of the elastic properties and intrinsic strength of monolayer graphene, Science 321, 38–388 (2008).
20. I. W. Frank, D. M. Tanenbaum, A. M. van der Zande, and P. L. McEuen, Mechanical properties of suspended graphene sheets, J. Vac. Sci. Technol. B 25, 2558–2561 (2007).
21. J. W. Suk, R. D. Piner, J. An, and R. S. Ruoff, Mechanical properties of monolayer graphene oxide, ACS Nano 4, 6557–6564 (2010).

22. H. M. Chien, M. C. Chuang, H. C. Tsai, H. W. Shiu, L. Y. Chang, C. H. Chen, S. W. Lee, J. D. White, and W. Y. Woon, on the nature of defects created on graphene by scanning probe lithography under ambient conditions, Carbon 80, 318–324 (2014).
23. J.L. Tsai, J.F. Tu, Characterizing mechanical properties of graphite using molecular dynamics simulation, Mater. *Des*, 31, 194-199 (2010).
24. Z. Ni, H. Bu, M. Zou, H. Yi, K. Bi, Y. Chen, Anisotropic mechanical properties of graphene sheets from molecular dynamics, *Physica B,* 405, 1301-1306 (2010).
25. A. Parashar, P. Mertiny, Representative volume element to estimate buckling behavior of graphene/polymer nanocomposites, Nanoscale Res. Lett., **7**, 515 (2012).
26. W. Wang, C. Shen, S. Li, J. Min, C. Yi, Mechanical properties of single layer graphene nanoribbons through bending experimental simulations, *AIP Advances,* 4, 031333 (2014).
27. A.Sakhaee-Pour, Elastic properties of single-layered graphene sheet, Solid State Commun., 149, 91-95 (2009).
28. H. M. Chien, M. C. Chuang, H. C. Tsai, H. W. Shiu, L. Y. Chang, C. H. Chen, S. W. Lee, J. D. White, and W. Y. Woon, on the nature of defects created on graphene by scanning probe lithography under ambient conditions, Carbon 80, 318–324 (2014).
29. A.G.Kvashnin, P.B.Sorokin, D.G.Kvashnin, The theoretical Study of Mechanical Properties of Graphene Membranes, Fullerenes Nanotubes Carbon Nanostruct, 18, 497-500 (2010).
30. M. M.Shokrieh, R. Rafiee, Prediction of Young's modulus of graphene sheets and carbon nanotubes using nanoscale continuum mechanics approach, *Mater. Des,* 31, 790-795 (2010).
31. J.R.Xiao, J.Staniszewski, J.W.Gillespie Jr., Fracture and progressive failure of defective graphene sheets and carbon nanotubes, *Compos. Struct*, 88, 602-609 (2009).
32. A. K. Geim and K. S. Novoselov, The rise of graphene, Nat.Mater. 6, 183–191 (2007).
33. A.Tapia, R.Peon-Escalante, C.Villanueva, F.Aviles, Influence of vacancies on the elastic properties of a graphene sheet, *Comput. Mater. Sci.*, 55, 255-262 (2012).
34. Web of science volume 7 numbers 11-21 march 2015 page 4587-5062
35. Rajasekeran G, Narayanan P and Parashar A 2016 Effect of point and line defects on mechanical and thermal properties of graphene: a review Crit. Rev. Solid State Mater. Sci.4147-71

36. Shao-Pei Wang, Jian-Gang Guo, Li-Jun Zhou, and Influence of Stone-Wales defects on elastic properties of graphene nanofilms, *Physica E*, 48, 29-35 (2013).
37. L. He, S. Guo, J. Lei, Z. Sha, Z. Liu, The effect of Stone-Thrower-Wales defects on mechanical properties of graphene sheets – A molecular dynamics study, *Carbon*, 75, 124-132 (2014).
38. M.C. Wang, C. Yan, L. Ma, N. Hu, M.W. Chen, and Effect of defects on fracture strength of graphene sheets, *Comput. Mater. Sci.*, 54, 236-239 (2012).
39. R.Ansari, S.Ajori, B.Motevalli, Mechanical properties of defective single-layered graphene sheets via molecular dynamics simulation, *Superlattices Microstruct.*, 51, 274-289 (2012).
40. J.R.Xiao, J.Staniszewski, J.W.Gillespie Jr., Fracture and progressive failure of defective graphene sheets and carbon nanotubes, *Compos. Struct.* 88, 602-609 (2009).
41. N. Jing, Q. Xue, C. Ling, M. Shan, T. Zhang, X. Zhou, Z. Jiao, Effect of defects on Young's modulus of graphene sheets: a molecular dynamics simulation, *RSC Adv.*, 2, 9124-9129 (2012).
42. Y.Y. Zhang a, Y. Cheng b, Q.X. Pei b, C.M. Wangc, Y. Xianga, Thermal conductivity of defective graphene, *Phys. Lett. A*, 376, 3668–3672 (2012).
43. Dewapriya, M. A. N., A. Srikantha Phani, and R. K. N. D. Rajapakse. "Effects of a Vacancy defect on Strength of Graphene Sheet and Carbon Nanotube."
44. Leyssale, Jean-Marc, and Gérard L. Vignoles. "A Large-Scale Molecular Dynamics Study of the Divacancy Defect in Graphene." The Journal of Physical Chemistry *C* 118, no. 15 (2014): 8200-8216.
45. Xiao, J. R., J. Staniszewski, and J. W. Gillespie. "Tensile behaviors of graphene sheets and carbon nanotubes with multiple Stone–Wales defects. *"*Materials Science and Engineering*:* A 527, no. 3 (2010): 715-723.
46. Rollings, E., G-H. Gweon, S. Y. Zhou, B. S. Mun, J. L. McChesney, B. S. Hussain, A. V. Fedorov, P. N. First, W. A. De Heer, and A. Lanzara. "Synthesis and characterization of atomically thin graphite films on a silicon carbide substrate." Journal of Physics and Chemistry of Solids 67, no. 9 (2006): 2172-2177.

47. Dervishi, Enkeleda, Zhongrui Li, Fumiya Watanabe, Abhijit Biswas, Yang Xu, Alexandru R. Biris, Viney Saini, and Alexandru S. Biris. "Large-scale graphene production by RF-CVD method." *Chem. Commun.* 27 (2009): 4061-4063.
48. S.Karmakar, Soumen, Naveen V. Kulkarni, Ashok B. Nawale, Niranjan P. Lalla, Ratikant Mishra, V. G. Sathe, S. V. Bhoraskar, and A. K. Das. "A novel approach towards selective bulk synthesis of few-layer graphenes in an electric arc." *Journal of Physics D: Applied Physics* 42, no. 11 (2009): 115201.
49. Jiao, Liying, Li Zhang, Xinran Wang, Georgi Diankov, and Hongjie Dai. "Narrow graphene nanoribbons from carbon nanotubes." Nature 458, no. 7240 (2009): 877-880.
50. Geim, A. K., and K. S. Novoselov. "The rise of graphene. Nature materials, 6: 183–191." (2007).
51. Kim, Hyunwoo, Ahmed A. Abdala, and Christopher W. Macosko. "Graphene/polymer nanocomposites." Macromolecules 43, no. 16 (2010): 6515-6530.
52. Bourlinos, Athanasios B., Vasilios Georgakilas, Radek Zboril, Theodore A. Steriotis, and Athanasios K. Stubos. "Liquid-Phase Exfoliation of Graphite towards Solubilized Graphenes." Small 5, no. 16 (2009): 1841-1845.
53. Stankovich, Sasha, Dmitriy A. Dikin, Richard D. Piner, Kevin A. Kohlhaas, Alfred Kleinhammes, Yuanyuan Jia, Yue Wu, SonBinh T. Nguyen, and Rodney S. Ruoff. "Synthesis of graphene-based nanosheets via chemical reduction of exfoliated graphite oxide." *Carbon* 45, no. 7 (2007): 1558-1565.
54. McAllister, Michael J., Je-Luen Li, Douglas H. Adamson, Hannes C. Schniepp, Ahmed A. Abdala, Jun Liu, Margarita Herrera-Alonso et al. "Single sheet functionalized graphene by oxidation and thermal expansion of graphite." Chemistry of Materials 19, no. 18 (2007): 4396-4404.
55. Schniepp, Hannes C., Je-Luen Li, Michael J. McAllister, Hiroaki Sai, Margarita Herrera-Alonso, Douglas H. Adamson, Robert K. Prud'homme, Roberto Car, Dudley A. Saville, and Ilhan A. Aksay. "Functionalized single graphene sheets derived from splitting graphite oxide." The Journal of Physical Chemistry B 110, no. 17 (2006): 8535-8539.
56. Lee, Changgu, Xiaoding Wei, Jeffrey W. Kysar, and James Hone. "Measurement of the elastic properties and intrinsic strength of monolayer graphene." science 321, no. 5887 (2008): 385-388.

57. E. Rollings, G. H. Gweon, S. Y. Zhou, B. S. Mun, J. L. McChesney, B. S. Hussain, A. Fedorov, P. N. First, W. A. de Heer, and A. Lanzara, "Synthesis and characterization of atomically thin graphite films on a silicon carbide substrate," J Phys Chem Solids 67 (9-10), 2172-2177 (2006).
58. C. Lee, X. Wei, J. W. Kysar, and J. Hone, "Measurement of the elastic properties and intrinsic strength of monolayer graphene," Science 321 (5887), 385-388 (2008).
59. E. Tkalya, M. Ghislandi, A. Alekseev, C. Koning, and J. Loos, "Latex-based concept for the preparation of graphene-based polymer nanocomposites," J Mater Chem 20 (15), 3035-3039 (2010).
60. H. Kim, Y. Miura, and C. W. Macosko, "Graphene/Polyurethane Nanocomposites for Improved Gas Barrier and Electrical Conductivity," Chem Mater 22 (11), 3441-3450 (2010).
61. S. Yadav, Z. Zhu, and C. V. Singh, Defect engineering of graphene for effective hydrogen storage, Int. J. Hydrog. Ener. 39, 4981–4995 (2014).
62. R. A. Quinlan, M. Cai, R. A. Outlaw, S. M. Butler, J. R. Miller, and A. N. Mansour, Investigation of defects generated in vertically oriented graphene, Carbon 64, 92–100 (2013).

63. A. Bosak, M. Krisch, M. Mohr, J. Maultzsch, and C. Thomsen, 1130 Elasticity of single-crystalline graphite: Inelastic x-ray scattering study, Phys. Rev. B Condens. Matter 75, 153408 (2007).
64. G. M. Odegard, T. S. Gates, L. M. Nicholson, and K. E. Wise, Equivalent-continuum modeling with application to carbon1495 nanotubes, NASA/TM-2002-211454.
65. E. Cadelano, P. L. Palla, S. Giordano, and L. Colombo, Nonlinear elasticity of monolayer graphene, Phys. Rev. Lett. 102, 1650235502 (2009).

66. J. Chen, M. Badioli, P. Alonso-Gonzalez, S. Thongrattanasiri, F. Huth, J. Osmond, M. Spasenovic, A. Centeno, A. Pesquera, P. Godignon, A. Zurutuza Elorza, N. Camara, F. J. G. de Abajo, R. Hillenbrand and F. H. L. Koppens, Nature, 2012, 487, 77–81.
67. Canadija, Marko, Marino Brcic, and Josip Brnic. "Bending behaviour of single-layered graphene nanosheets with vacancy defects." Engineering Review 33, no. 1 (2013): 9-14.

68. C. Sevik, H. Sevincli, G. Cuniberti, and T. Cagin, Phonon engineering in carbon nanotubes by controlling defect concentration, Nano Lett. 11, 4971–4977 (2011).
69. R. A. Quinlan, M. Cai, R. A. Outlaw, S. M. Butler, J. R. Miller, and A. N. Mansour, Investigation of defects generated in vertically oriented graphene, Carbon 64, 92–100 (2013).
70. Jing, Nuannuan, Qingzhong Xue, Cuicui Ling, Meixia Shan, Teng Zhang, Xiaoyan Zhou, and Zhiyong Jiao. "Effect of defects on Young's modulus of graphene sheets: a molecular dynamics simulation." Rsc Advances 2, no. 24 (2012): 9124-9129.
71. Zhu, Jian, Ming He, and Feng Qiu. "Effect of Vacancy Defects on the Young's Modulus and Fracture Strength of Graphene: A Molecular Dynamics Study." Chinese Journal of Chemistry 30, no. 7 (2012): 1399-1404.
72. Parashar, Avinash, and Pierre Mertiny. "Study of mode I fracture of graphene sheets using atomistic based finite element modeling and virtual crack closure technique." International Journal of Fracture 176, no. 1 (2012): 119-126.
73. Gorjizadeh, N., Farajian, A. A., & Kawazoe, Y. (2009). The effects of defects on the conductance of graphene nanoribbons. Nanotechnology, 20(1), 015201.
74. Banhart, Florian, Jani Kotakoski, and Arkady V. Krasheninnikov. "Structural defects in graphene." ACS nano 5, no. 1 (2010): 26-41.
75. Xu, Lanqing, Ning Wei, and Yongping Zheng. "Mechanical properties of highly defective graphene: from brittle rupture to ductile fracture. "Nanotechnology 24, no. 50 (2013): 505703
76. T. Zhang, X. Li, and H. Gao, Designing graphene structure with controlled distributions of topological defects: A case study of toughness enhancement in graphene ruga, Extreme Mech. Lett. http://dx.doi.org/10.1016/j.eml.2014.12.007 (2015).
77. E. Rollings, G. H. Gweon, S. Y. Zhou, B. S. Mun, J. L. McChesney, B. S. Hussain, A. Fedorov, P. N. First, W. A. de Heer, and A. Lanzara, "Synthesis and characterization of atomically thin graphite films on a silicon carbide substrate," J Phys Chem Solids 67 (9-10), 2172-2177 (2006).

78. N. Chandra, S. Namilae, and C. Shet, Local elastic properties of carbon nanotubes in the presence of Stone-Wales defects, Phys.Rev. B Condens. Matter 69, 094101 (2004).
79. Ito, Akihiko, and Shingo Okamoto. "Mechanical properties of vacancy-containing graphene and graphite using molecular dynamics simulations." In Proceedings of the International Multi Conference of Engineers and Computer Scientists, vol. 1. 2012.
80. S. J. Stuart, A. B. Tutein, and J. A. Harrison, A reactive potential for hydrocarbons with intermolecular interactions, J. Chem.Phys. 112(14), 6472–6486 (2000).
81. . Q. X. Pei, Y. W. Zhang, and V. B. Shenoy, A molecular dynamics study of the mechanical properties of hydrogen functionalized graphene, Carbon 48, 898–904 (2010).
82. N. Chandra, S. Namilae, and C. Shet, Local elastic properties of carbon nanotubes in the presence of Stone-Wales defects, Phys.Rev. B Condens. Matter 69, 094101 (2004).
83. Rahul P Hardikar, Atanu Samanta, Aaditya Manjanath and Abhishek K. Singh, Vacancy mediated clipping of multi layered graphene: A precursor for 1,2 and 3D carbon structures, Carbon 94 (2015) 67-72.